PaleoBios 35: 1–22, December 24, 2018

PaleoBios

OFFICIAL PUBLICATION OF THE UNIVERSITY OF CALIFORNIA MUSEUM OF PALEONTOLOGY

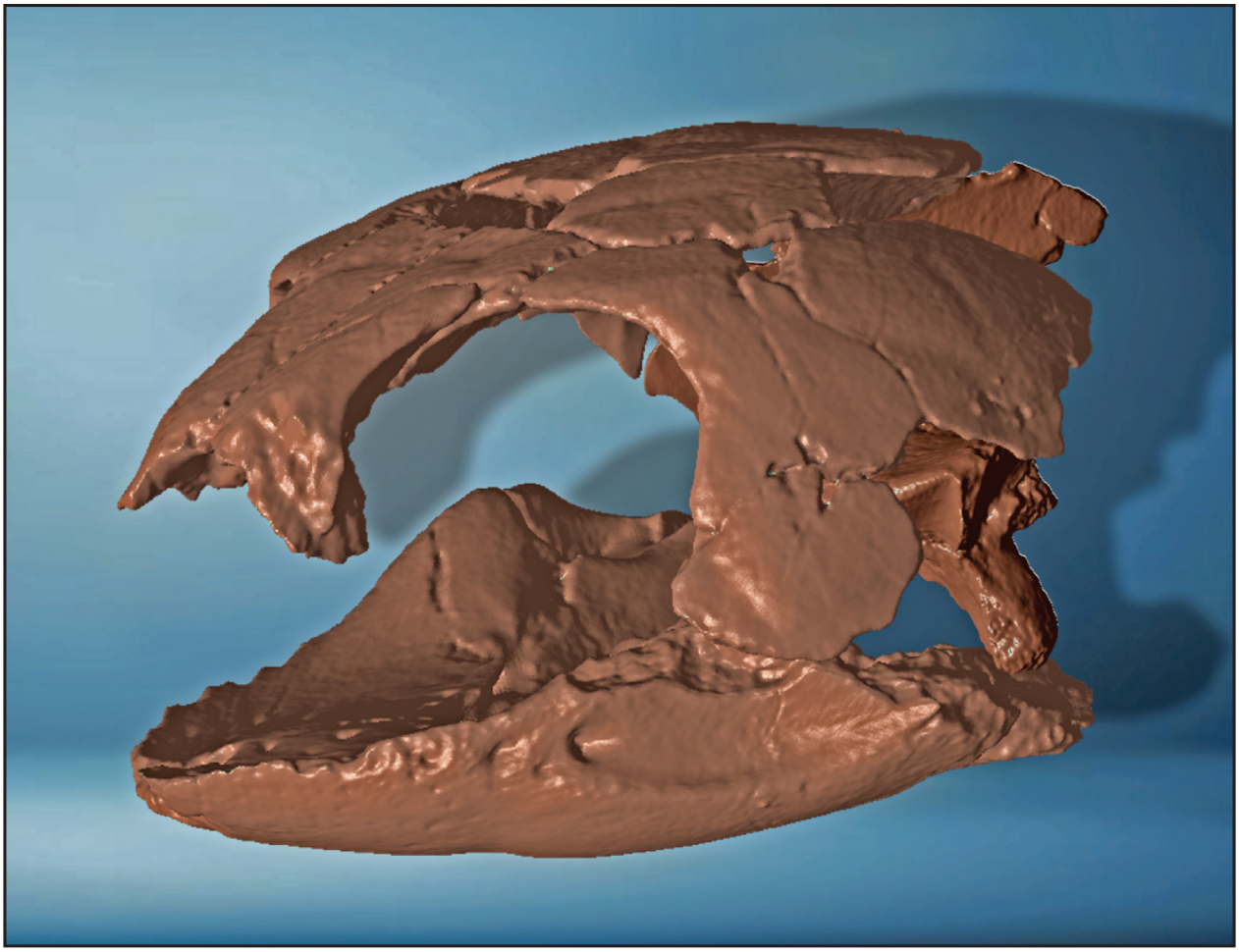

PAUL V. ULLMANN, ZACHARY M. BOLES & MICHAEL J. KNELL (2018). Insights into cranial morphology and intraspecific variation from a new subadult specimen of the pan-cheloniid turtle *Euclastes wielandi* Hay, 1908.

Cover illustration: Laser scans of the partial skull and mandible of *Euclastes wielandi*, specimen RU-EFP-00009.
Citation: Ullmann, P.V., Z.M. Boles and M.J. Knell. 2018. Insights into cranial morphology and intraspecific variation from a new subadult specimen of the pan-cheloniid turtle *Euclastes wielandi* Hay, 1908. *PaleoBios*, 35. ucmp_paleobios_42081.

Insights into cranial morphology and intraspecific variation from a new subadult specimen of the pan-cheloniid turtle *Euclastes wielandi* Hay, 1908

PAUL V. ULLMANN[1*], ZACHARY M. BOLES[1], AND MICHAEL J. KNELL[2]
[1]Department of Geology, Rowan University, 201 Mullica Hill Road, Glassboro, New Jersey 08028, USA; *ullmann@rowan.edu*; *bolesz@rowan.edu*
[2]Department of Earth Science, Southern Connecticut State University, 501 Crescent Street, New Haven, Connecticut 06515, USA; *knellm1@southernct.edu*

We describe a nearly complete skull and mandible of a subadult of *Euclastes wielandi*, a pan-cheloniid turtle recently recovered at the Jean and Ric Edelman Fossil Park at Rowan University in Mantua Township, New Jersey, which yields new information about the osteology, ontogeny, and intraspecific variation of this taxon. The specimen was collected from the earliest Danian Main Fossiliferous Layer (MFL) of the Hornerstown Formation. Although discovered immediately adjacent to remains of two pleurodires, *Taphrosphys sulcatus* and *Bothremys* sp., the skull and mandible can be definitively assigned to Pan-Cheloniidae based on its V-shaped basisphenoid and rod-like rostrum basisphenoidale. Among three pan-cheloniid taxa known from the MFL, the specimen is assigned to *Eu. wielandi* based on its low skull with dorsally-directed orbits, symphyseal swelling in the mandibular triturating surface, and high dorsum sellae. Comparisons with other specimens of *Eu. wielandi* and adults and juveniles of other pan-cheloniids revealed variations in the type and timing of cranial ontogenetic changes in the clade, as well as anatomical traits subject to intraspecific variation, such as the depth of the sella turcica, paths of the foramina nervi hypoglossi, and development of a precolumellar fossa. The relative contribution of the frontal to the orbital margin and precise path of the prefrontal-supraorbital scale sulcus are subject to individual variation in *Eu. wielandi*, as well as ontogenetic variation and bilateral asymmetry in other cryptodirans, signifying that the widespread use of frontal retraction in taxon diagnoses and as a phylogenetic character should be reconsidered. As in multiple other taxa, the mandibular triturating surface expands through growth in *Eu. wielandi*, demonstrating that increased durophagy with age was a common life strategy among Cryptodira.

Keywords: *Euclastes*, Chelonioidea, turtle, intraspecific variation, cranial morphology, Edelman Fossil Park

INTRODUCTION

Shallow marine glauconitic greensands along the Cretaceous through Paleocene coastal plain deposits of New Jersey have been a focus in vertebrate paleontology since nearly the beginnings of the discipline in North America. Since the discovery within these sediments of *Hadrosaurus foulkii* Leidy, 1858, the first relatively complete dinosaur (Prieto-Marquez et al. 2006), paleontologists have encountered prolific assemblages of diverse Cretaceous and Paleocene faunas. These faunas comprise a rich suite of primarily shallow-marine and paralic invertebrates and vertebrates, including turtles, birds, crocodilians, fish, sharks, rays, and occasional bloat-and-float dinosaur material (Gallagher 1991, 1993, 2003). Vertebrate fossils are especially abundant from the time span recorded by the Maastrichtian Navesink through Thanetian Vincentown formations, a sequence of glauconitic greensand deposits that are best exposed at Jean and Ric Edelman Fossil Park (formerly the Inversand Mining Company pit) in Mantua Township, New Jersey (Fig. 1). By far the richest fossil bearing unit in this sequence is the "Main Fossiliferous Layer", the MFL, near the base of the Maastrichtian–Danian Hornerstown Formation (Gallagher 1993, 2003). This bonebed is at the focus of ongoing paleontological research due to its complex taphonomic history. Recent analyses by Obasi et al. (2011) and Esmeray-Senlet et al. (2017) at Edelman Fossil Park encountered shocked quartz within an in-filled burrow immediately underlying the MFL and an iridium spike within the MFL, indicating that the MFL may represent a thanatocoenosis related to ecosystem collapse immediately following the Chicxulub impact (Obasi et al. 2011, Boles 2016).

Turtles are perhaps the most common larger vertebrates

*author for correspondence

Citation: Ullmann, P.V., Z.M. Boles and M.J. Knell. 2018. Insights into cranial morphology and intraspecific variation from a new subadult specimen of the pan-cheloniid turtle *Euclastes wielandi* Hay, 1908. *PaleoBios*, 35. ucmp_paleobios_42081.
Permalink: https://escholarship.org/uc/item/8dw67415

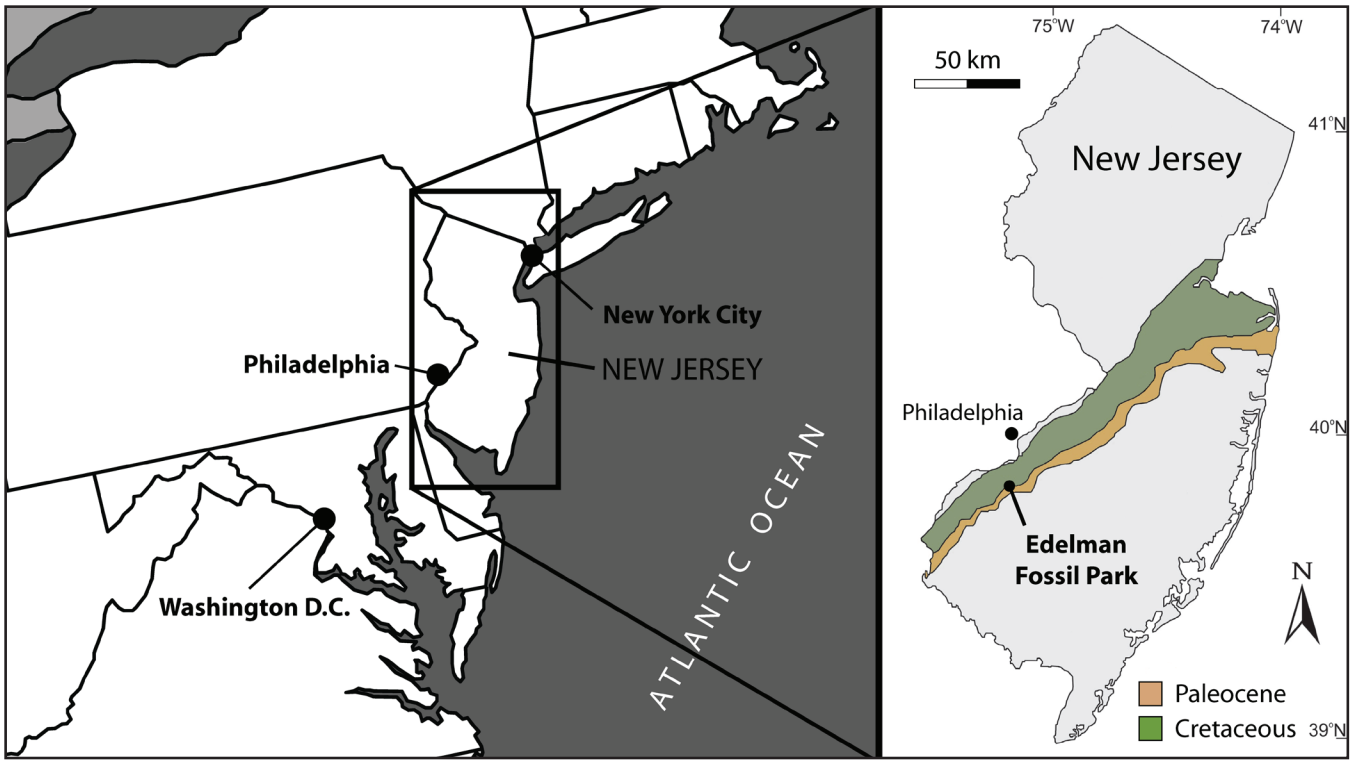

Figure 1. Location map for Edelman Fossil Park. Inset at right includes outcrop of Cretaceous and Paleocene strata in New Jersey. Scale as indicated. New Jersey inset map modified with permission from Horner et al. (2016).

in the MFL, with five marine-adapted taxa currently known: *Bothremys* sp. Leidy, 1865, *Catapleura repanda* Cope, 1868b, *Euclastes wielandi* Hay, 1908, *Peritresius ornatus* Leidy, 1856, and *Taphrosphys sulcatus* Leidy, 1856 (Gallagher 2003). Knowledge of MFL turtles has been coalesced in a piecemeal fashion from numerous fragmentary specimens (e.g., Hay 1908, Gaffney 1975, Parris et al. 1986, Parham 2005, Hirayama 2006, Ullmann et al. in press), which are likely an unfortunate consequence of "bloat and float" decay (Schwimmer, 1997; Boles, 2016), intense bioturbation (Gallagher 2003, Obasi et al. 2011), and potential collection biases in earlier decades (Baird 1964, Denton et al. 1997). A case in point is specimen RU-EFP-00009, which we describe here as the remains of a subadult *Eu. wielandi.* It was originally interpreted by Ullmann and Lacovara (2011) to belong to the pleurodire *Ta. sulcatus* as it was found only a few decimeters away from a plastron and partial carapace of an individual definitively identified as *T. sulcatus* (Ullmann et al. in press). RU-EFP-00009 was also found immediately adjacent to poorly preserved and fragmentary remains of another, smaller turtle, *Bothremys* sp., further complicating the delineation of elements to individuals (Ullmann and Lacovara 2011). However, the overlap in skeletal representation and detailed osteologic comparisons definitively differentiate RU-EFP-00009 from each of these pleurodires. Based on the presence of multiple chelonioid and pan-cheloniid synapomorphies and autapomorphies of *Euclastes*, it is now clear that the partial skull and mandible are those of a subadult of *Eu. wielandi*. In addition, we discuss aspects of ontogenetic and individual variation in cranial morphology in modern and fossil turtles.

MATERIALS AND METHODS

The skull and mandible of RU-EFP-00009 described in this study were recovered during fieldwork at Edelman Fossil Park in 2010. RU-EFP-00009 comprises a partial skull roof that preserves both prefrontals, frontals, and postorbitals, much of both parietals, a fragment of the left jugal, and a fragment of the right maxilla (Fig. 2). The preserved braincase is comprised of the supraoccipital, both prootics and opisthotics, the left exoccipital, left quadrate, fragments of both pterygoids, the basisphenoid, and the basioccipital (Fig. 3). The morphology of a complete lower jaw can be described when both rami and dentaries are taken into account (Fig. 4): essentially all portions missing from one side are present on the other side.

In this paper we use the anatomical nomenclature

of Gaffney (1972, 1979) and follow the written format of Gaffney et al. (2006): (1) element name; (2) its preservation state; (3) contacts; and (4) structures. Lack of suture fusion for all elements (except between the right prefrontal and frontal) allows the precise extent of each element to be discerned.

Character numbers and their state are boldfaced in the text, with the character number cited first followed by the state, the two separated by a colon (e.g., **132:2**). Characters and states follow Evers and Benson 2018.

Institutional abbreviations—AMNH, American Museum of Natural History, New York, New York; **IGPS**, Institut für Geologie und Paläontologie der Universität Salzburg, Salzburg, Austria; **NJSM**, New Jersey State Museum, Trenton, New Jersey; **RU-EFP**, Jean and Ric Edelman Fossil Park at Rowan University, Glassboro, New Jersey.

SYSTEMATIC PALEONTOLOGY

TESTUDINES Batsch, 1788
CRYPTODIRA Cope, 1868a
CHELONIOIDEA Baur, 1893
PAN-CHELONIIDAE Joyce, Parham & Gauthier 2004
EUCLASTES Cope, 1867
EUCLASTES WIELANDI Hay, 1908
Figs. 2–4

Material—RU-EFP-00009, a nearly complete skull roof (Fig. 2), braincase (Fig. 3), and lower jaw (Fig. 4).

Occurrence—RU-EFP-00009 was discovered in the Main Fossiliferous Layer (MFL) near the base of the glauconite-rich, Maastrichtian–Danian Hornerstown Formation at Jean and Ric Edelman Fossil Park at Rowan University, Mantua Township, New Jersey. As reviewed by Gallagher (1993, 2003), the MFL is an assemblage of diverse shallow marine vertebrate and invertebrate fossils, which Obasi et al. (2011) suggest may be attributable to a thanatocoenosis resulting from the Chicxulub impact.

DESCRIPTION AND COMPARISONS

Cranial scale sulci

Scale sulci are visible on the skull roof, and they generally conform to the geometry of scale sulci in other specimens of *Euclastes* (Fastovsky 1985, Hirayama and Tong 2003, Jalil et al. 2009). A pair of prefrontal scales meet along the midline and extend laterally to the margin of the orbit. Unlike other specimens of *Eu. wielandi* (NJSM 11872 [Fastovsky 1985], AMNH 30030, and AMNH 30022 [Hirayama and Tong 2003]), the prefrontal-supraorbital sulcus crosses the posterior end of the prefrontal to the margin of the orbit (rather than meeting the orbit margin on the frontal). A single, anteriorly-rectangular frontal scale is positioned sagittally posterior to it; the posterior shape of this scale cannot be determined due to missing bone. A small, hexagonal scale occurs posterior to the frontal scale along the midline, between the arcuate, posterolaterally-angled frontoparietal scales. Termed the parietal 1 scale by Jalil et al. (2009), this "additional" scale (*sensu* Tong and Hirayama 2008) is elsewhere known in *Eu. acutirostris* Jalil et al., 2009, *Erquelinnesia gosseleti* Zangerl, 1971, *Argillochelys africana* Tong and Hirayama, 2008, and other specimens of *Eu. wielandi* (Fastovsky 1985, Hirayama and Tong 2003). The parietal 2 scale of Jalil et al. (2009) spans the midline posterior to this scale; its anterior margin is rectangular. The parasagittal parietal scales are anteroposteriorly long, rectangular, and each terminate anteriorly in an apex. Laterally, the supraorbital scales are large with rounded margins. They posteriorly abut large, semi-rectangular temporal scales. The dorsal extent of the jugal scale would have covered the lateral face of the postorbital.

Prefrontal

Preservation—Both prefrontals lack the ventral margin of the element forming the posterior wall of the fossa nasalis, lateral to the opening of the fissura ethmoidalis; they are otherwise complete.

Contacts—As preserved, the right prefrontal is fused to the right frontal; the suture between these elements is partially closed (as defined by Bailleul et al., 2016) (Fig. 2A). All other sutural contacts in the skull roof, including the symphysis between the prefrontals, were glued during preparation. The prefrontal contacts the maxilla anteriorly and the frontal posteriorly. Due to loss of the ventral margin of the ventral process of each prefrontal, it cannot be determined if they contacted the palatine. A thin contribution of the frontal to the orbit precludes contact between the prefrontal and postorbital. In dorsal view, the maxilla-prefrontal suture forms a concave-forward arc, which does not reach the midline (Fig. 2A, D). The prefrontal-frontal suture is long, nearly straight in dorsal and ventral views, and angled anteromedially-posteromedially due to development of the anterior frontal processes (Fig. 2A, B, D, E). No nasals are present, resembling the condition in *Euclastes* (Fastovsky 1985).

Structures—The prefrontal forms a narrow contribution to the posterodorsal margin of the apertura narium externa. Lateral to the fissura ethmoidalis, the ventral projections of each prefrontal form rounded right angles, which represent the posterodorsolateral corners of the

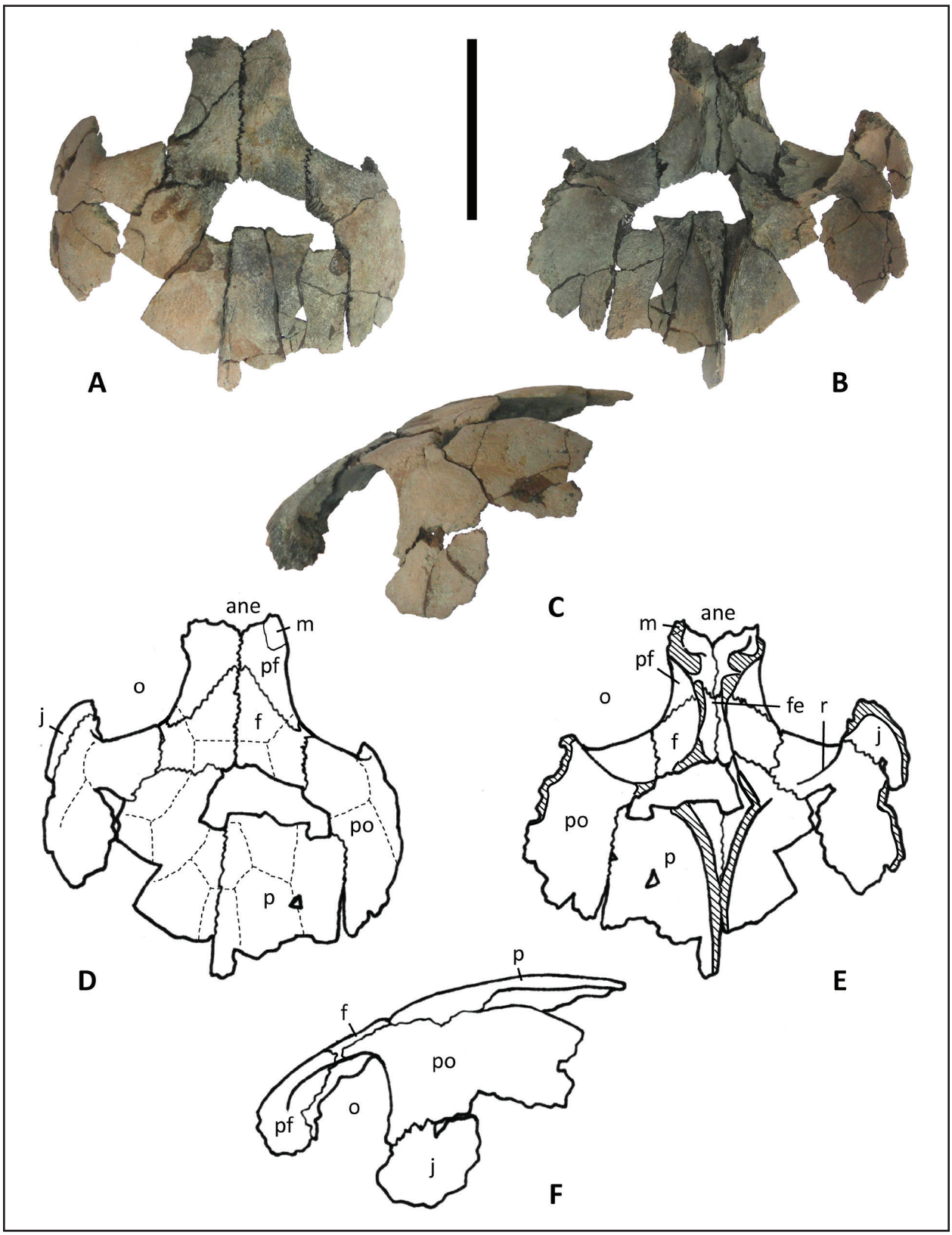

Figure 2. Skull roof of *Euclastes wielandi*, RU-EFP-00009. Specimen and line drawings, respectively, in dorsal (**A**, **D**), ventral (**B**, **E**), and left lateral views (**C**, **F**). Anterior towards top in (**A**–**B**) and (**D**–**E**). Cranial scale sulci are shown in (**D**) as dashed lines. **Abbreviations**: **ane**, apertura narium externa; **f**, frontal; **fe**, fissura ethmoidalis; **j**, jugal; **m**, maxilla; **o**, orbit; **p**, parietal; **pf**, prefrontal; **po**, postorbital; **r**, ridge. Hashing indicates broken and/or eroded surfaces. Scale bar=5 cm.

fossa nasalis (Fig. 2B, E). The ventral walls forming the posterior wall of the fossa nasalis are well developed, as in other cryptodires (Gaffney 1979), being equally as thick as the anterior projection of the bone contacting the maxilla. A sharp keel is present along the lateral margin of the prefrontal, along the entire length of its contribution to the orbit. Two neurovascular foramina are present on the ventral surface of each prefrontal, posterolateral to the opening of the fissura ethmoidalis.

Frontal

Preservation—Both frontals are complete, except for the thin, ventral edge of the parasagittal wall of bone laterally bounding the sulcus olfactorius and forming the dorsal margin of the foramen interorbitale.

Contacts—The frontal contacts the prefrontal anteriorly, the postorbital posterolaterally, and the parietal posteriorly. The contact with the postorbital is shorter than the suture with the parietal. These two, straight sutures meet at nearly a right angle, giving the frontal a square form posteriorly (Fig. 2A, D).

Structures—The frontals exhibit strongly developed anterior processes along the midline, as in many other chelonioids (e.g., *Cabindachelys landanensis* Myers et al., 2017; *Argillochelys africana* Tong and Hirayama, 2008). At the posterior end of the prefrontal-frontal contact in dorsal view, the suture takes a short but abrupt turn anteriorly. This turn forms the anterior margin of a thin, lateral bar of the frontal, which provides a very short contribution to the orbital margin (Fig. 2A, B, D, E). This is similar to the condition in *Eu. acutirostris* (Jalil et al. 2009, fig. 3) and *Procolpochelys charlestonensis* Weems and Brown, 2017 (Weems and Brown 2017, fig. 2) but contrasts the condition in the larger skull of NJSM 11872 of *Eu. wielandi*, in which the frontal provides a broad contribution to the orbital margin (Fastovsky 1985); variation in this feature among turtles is reviewed in greater detail in the Discussion. Ventrally, each frontal exhibits a parasagittal ridge close to the midline, which progressively turns posterolaterally near the posterior margin of the bone. This ridge continues onto the prefrontal anteriorly and the parietal posteriorly (Fig. 2B, E), and when articulated in the skull, the ridges formed sheets of bone beside the sulcus olfactorius along the midline. A small neurovascular foramen is present on the ventral surface of each frontal, laterally adjacent to the parasagittal ridge near the anteroposterior midpoint of each bone.

Parietal

Preservation—Portions of both parietals are preserved, but neither is complete. Both parietals are missing the posterior end/margin. The right parietal is also missing its anterior end and processus inferior parietalis, and the left parietal is also missing the majority of its posterolateral extent, its anteromedial corner, and the anteroventral portion of the processus inferior parietalis.

Contacts—As preserved, the parietal contacts the frontal anteriorly, the postorbital laterally, the prootic posteroventrally along the processus inferior parietalis, and the supraoccipital posteroventrally along the midline of the skull roof; contact with the squamosal is uncertain in this specimen due to lack of preservation of the posterior portion of each parietal. The parietal-postorbital suture gently curves anteromedially whereas all other sutures bounding the parietal are nearly straight in dorsal view (Fig. 2A, D). This arrangement gives the anterolateral margin of the parietal a broadly rounded shape.

Structures—The parietal is long anteroposteriorly and gradually becomes dorsoventrally thinner toward the posterior end of the element. It is slightly convex dorsally in posterior view. The anterodorsal portion of the processus inferior parietalis extends anteriorly underneath the main plate of the frontal, forming a triangular-in-cross-section suture surface. A broken ridge of bone is present along the midline margin of the ventral surface of each parietal along the posterior half of the bone (Fig. 2B, E); these ridges, abut against each other when articulated, and unite with the dorsal margin of the crista supraoccipitalis. These ridges curve anterolaterally to merge into the base of each processus inferior parietalis, enclosing the cavum cranii between them along the midline. The ventral-most preserved portion of the processus inferior parietalis comprises a mediolaterally thin, parasagittally oriented wall (Fig. 3B, G), the posterior border of which forms the anterior border of the closed foramen nervi trigemini. Unlike *Chelonia* Linnaeus, 1758 (Gaffney 1979), the foramen nervi trigemini is not divided by a ventral process from the parietal.

Jugal

Preservation—A fragment of the dorsolateral portion of the left jugal is preserved, posterior to the orbit.

Contacts—The fragment is bound dorsally by a convex suture to the postorbital (Fig. 2F); no other contacts can be discerned.

Structures—Though the anterior margin of the fragment is weathered, it appears (based on breadth) that it would have contributed to the margin of the orbit. The anterior third of the fragment gradually thickens mediolaterally.

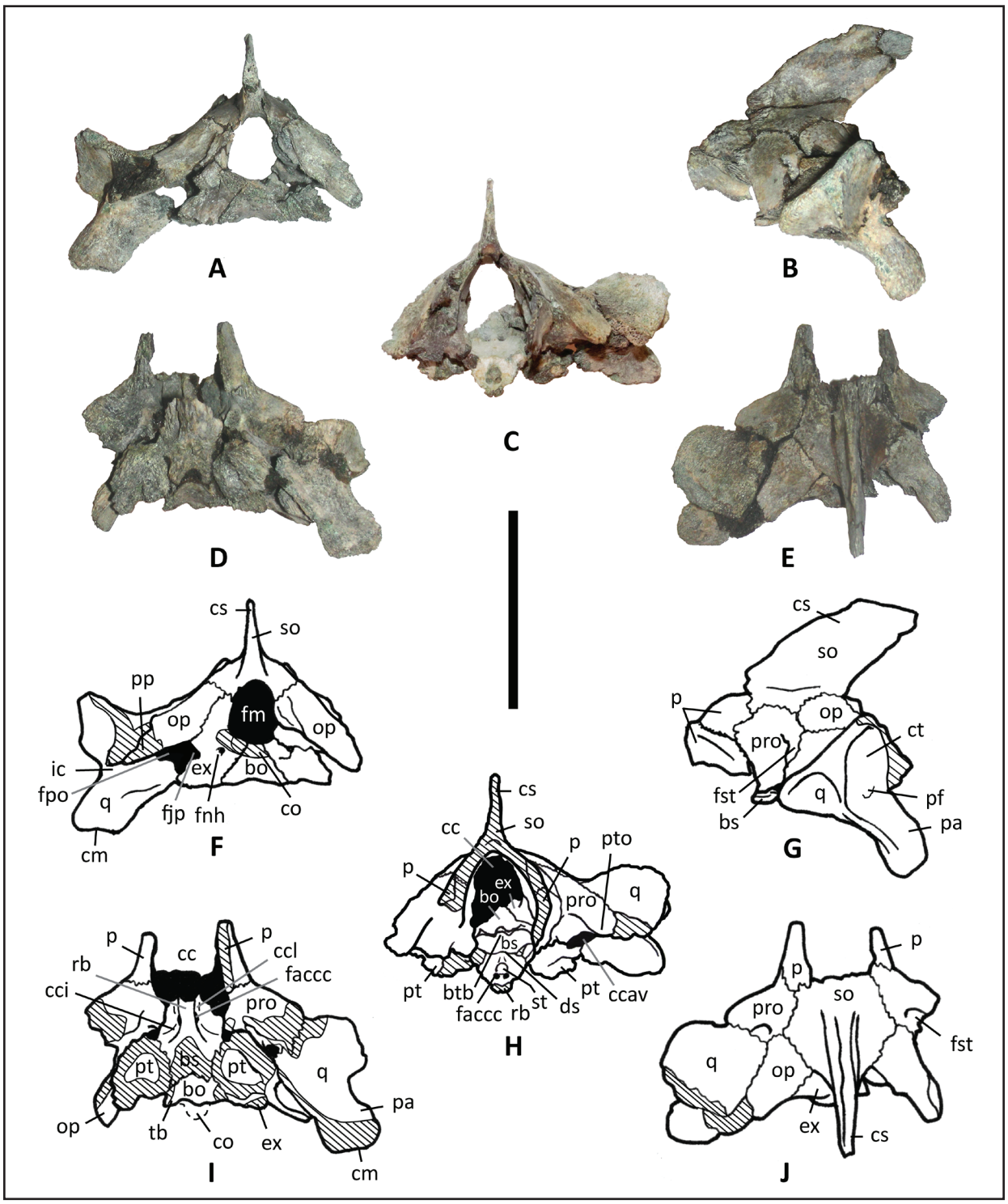

Figure 3. Braincase of *Euclastes wielandi,* RU-EFP-00009. Specimen and line drawings, respectively, in posterior (**A, F**), left lateral (**B, G**), anterior (**C, H**), ventral (**D, I**), and dorsal views (**E, J**). Anterior towards top in (**D, E**) and (**I, J**). **Abbreviations**: **bo**, basioccipital; **bs**, basisphenoid; **btb**, basis tuberculum basalis; **cc**, cavum cranii; **ccav**, canalis cavernosus; **cci**, canalis caroticus internus; **ccl**, canalis caroticus lateralis; **cm**, condylus mandibularis; **co**, condylus occipitalis; **cs**, crista supraoccipitalis; **ct**, cavum tympani; **ds**, dorsum sellae; **ex**, exoccipital; **faccc**, foramen anterius canalis carotici cerebralis; **fjp**, foramen jugulare posterius; **fm**, foramen magnum; **fnh**, foramen nervi hypoglossi; **fpo**, fenestra postotica; **fst**, foramen stapedio-temporale; **ic**, incisura columellae auris; **op**, opisthotic; **p**, parietal; **pa**, processus articularis; **pf**, precolumellar fossa; **pp**, processus paraoccipitalis; **pro**, prootic; **pt**, pterygoid; **pto**, processus trochlearis oticum; **q**, quadrate; **rb**, rostrum basisphenoidale; **so**, supraoccipital; **sq,** squamosal; **st**, sella turcica; **tb**, tuberculum basioccipitale. Hashing indicates broken and/or eroded surfaces. Scale bar=5 cm.

Postorbital

Preservation—The ventrolateral edges and posterior ends of both postorbitals are missing. Although the left postorbital is less complete than the right postorbital, it preserves the complete ridge defining the posterior margin of the fossa orbitalis (whereas the anterolateral end of this ridge is incomplete in the right element).

Contacts—As preserved, the postorbital contacts the frontal anteromedially, the parietal posteromedially, and the jugal ventrally; contact with the squamosal cannot be discerned due to incompleteness of the posterolateral region of each postorbital. The contact with the parietal is long and nearly straight in its posterior half (Fig. 2A, B, D, E). Missing fragments of the right parietal expose the postorbital-parietal suture surface on this side of the skull, showing that the parietal would have dorsally overlapped the postorbital along this suture.

Structures—The postorbital forms the vast majority of the posterodorsal margin of the orbit. Ventrally, a sharp, ventrally-keeled, mediolaterally-oriented ridge divides the fossa orbitalis from the fossa temporalis inferior near the anterior margin of the element (labeled "r" in Fig. 2E). This ridge is low, angled slightly posteromedially-anterolaterally in ventral view, and becomes more defined and more sharply keeled anterolaterally, as in most cryptodires (in contrast to the development of this ridge into a complete wall in trionychids and pleurodires; Gaffney 1979). The thickness of the postorbital is greatest at the position of this ridge, and, similar to the parietal, the right postorbital shows that the element becomes very thin near its posterior end. The orbital margin is keeled to a similar degree as seen on the prefrontal.

Maxilla

Preservation—Only a very small fragment of the right maxilla is preserved, which is weakly sutured to the right prefrontal (Fig. 2A, D). The contact surface on the left prefrontal for articulation with the left maxilla is exposed, forming an anterodorsolaterally oriented surface.

Quadrate

Preservation—The left quadrate is preserved and mostly complete. Its posterodorsal margins are weathered, including the region of articulation to the squamosal. It is also missing its anterodorsal corner, the medial tip of the processus epipterygoideus, the edge of its dorsoventrally-oriented lateral ridge, and the articular surface of the condylus mandibularis. The dorsal surface of the bone is highly porous and exhibits a fibrous surface texture with fine lineations angled parallel to the contact with the opisthotic.

Contacts—As preserved, the left quadrate contacts the prootic anteromedially, the opisthotic posteromedially, and the pterygoid ventromedially. In dorsal view, the quadrate-prootic and quadrate-opisthotic sutures are approximately equal in length, straight, and meet at roughly a right angle that points medially (Fig. 3E, J). The suture surface for the pterygoid is exposed ventrally (due to this portion of the left pterygoid being missing). This surface is formed by two planes: a posterior horizontal plane that runs into a vertical, anteriorly-positioned plane. Both planes exhibit straight suture lineations.

Structures—Incompleteness of the anterodorsal corner of the quadrate precludes determination of whether or not it contributed to the processus trochlearis oticum. In dorsal view, the quadrate and prootic form roughly equal contributions to the border of the foramen stapedio-temporale, with the quadrate making up the posterolateral half of its margin along the suture to the prootic (Fig. 3E, J). The incisura columellae auris is open posteriorly, contrasting the fully enclosed condition in *Chelydra serpentina* Linnaeus, 1758 (Gaffney 1972, 1979). It crosses the middle of the posterior face of the quadrate as a mediolaterally oriented groove (Fig. 3A, F). In lateral view, its cross section is semicircular, and just anterior to its lateral entrance is a small, conical depression within the cavum tympani (Fig. 3B, G); this concavity has been termed the precolumellar fossa by Williams (1954, p. 286). The anterior border of the cavum tympani is defined by a weakly sigmoid, dorsoventrally-oriented ridge of bone traversing the lateral face of the quadrate. This ridge dissipates into the anterolateral margin of the processus articularis distally, which is long, ventrolaterally directed, and rectangular in cross section (i.e., in ventral view; Fig. 3D, I). We could not determine if the canalis chorda tympani quadrati is present due to poor preservation of the surface texture on the posterior face of the processus articularis (obscuring identification of the foramen chorda tympani inferius if it is present) and inability to view all surfaces within the cavum acustico-jugulare (to identify whether or not a foramen chorda tympani superius is present). Presence of the chorda tympani quadrati is subject to bilateral and possibly ontogenetic variation in *Ctenochelys* Hay, 1905 (Matzke 2007) and to sexual dimorphism in the kinosternid *Sternotherus* Gray, 1825 (Bever 2009a), so it remains unclear whether or not its presence should be expected in a subadult *Euclastes*. However, there are no clear pores filled with sediment in the posterior face of the processus articularis, suggesting the foramen

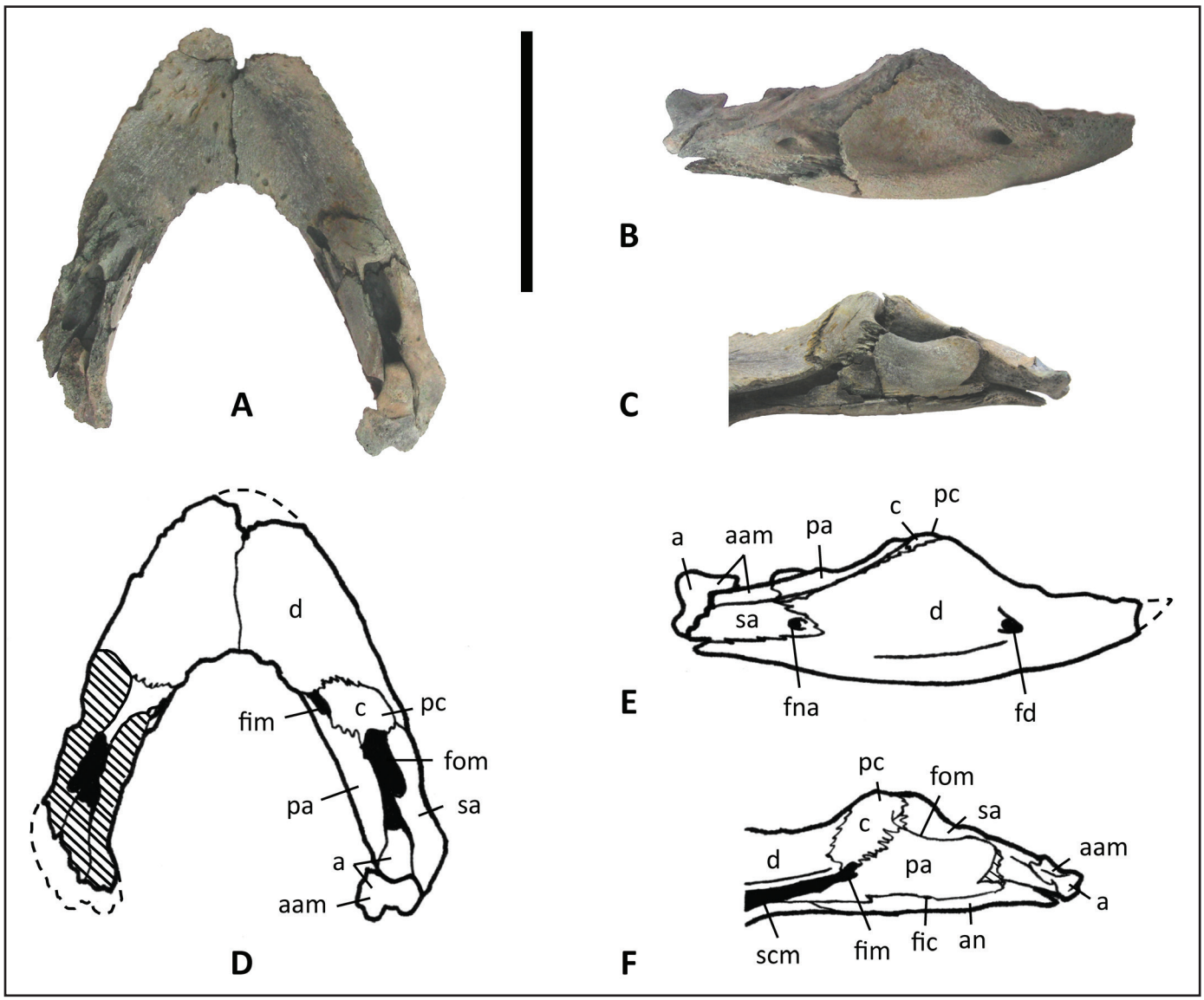

Figure 4. Mandible of *Euclastes wielandi*, RU-EFP-00009. Specimen and line drawings, respectively, in dorsal (**A, D**) and right lateral (**B, E**) views, including medial view of right mandibular ramus (**C, F**). **Abbreviations**: **a**, articular; **aam**, area articularis mandibularis; **an**, angular; **c**, coronoid; **d**, dentary; **fd**, foramen dentofaciale majus; **fic**, foramen intermandibularis caudalis; **fim**, foramen intermandibularis medius; **fna**, foramen nervi auriculotemporalis; **fom**, fossa meckelii; **pa**, prearticular; **pc**, processus coronoideus; **sa**, surangular; **scm**, sulcus cartilaginis meckelii. Hashing indicates broken and/or eroded surfaces. Scale bar=5 cm.

chorda tympani inferius may have been absent (this would match the condition in extant cheloniids; Gaffney 1979). Medially, the incisura columellae auris opens into the cavum acustico-jugulare, the lateral wall of which is formed by the quadrate. Just anterior to this point, the embayment diverges into two anteriorly-directed grooves in the medial face of the quadrate dorsal to the processus epipterygoideus. The more dorsal of these two grooves is the canalis stapedio-temporalis and the ventral groove is the canalis cavernosus (Gaffney 1972, 1979). They are roughly equal in diameter.

Pterygoid

Preservation—Only a fragment of the central portion of each pterygoid is preserved. The ventral surface of the fragment of the left pterygoid is intact, but this surface is missing from the right element.

Contacts—The preserved fragments contact the prootic dorsally, the basisphenoid medially, the basioccipital posteromedially, the exoccipital posteriorly, and the quadrate laterally. A large, triangular suture surface on the left quadrate demonstrates that a long, posterolateral extension of the pterygoid is missing.

Structures—Although the foramen posterius canalis carotici interni is not intact, in posteroventral view the canalis caroticus internus can be seen passing anterodorsally through the body of the coracoid to the dorsomedial surface of the pterygoid. This canal is angled slightly medially through the pterygoid and is entirely encased by it, as in cheloniids and *Macrochelys* (Gaffney 1979). This condition contrasts that of *Chelydra*, in which the roof of the canal is partly formed by the prootic (Gaffney 1979). The canalis cavernosus, occupied in life by the lateral head vein, is present over the dorsal surface of each preserved pterygoid fragment, as in most cryptodires (Gaffney 1979). This canal is distinctly larger in diameter than the canalis caroticus internus and, though also passing posterolaterally-anteromedially, it is oriented more mediolaterally. The pterygoid forms a small portion of the ventral border of the foramen cavernosum at the posterior end of the canalis cavernosus.

Supraoccipital

Preservation—The supraoccipital is complete. Two parasagittal cracks on either side of the base of the crista supraoccipitalis have been glued during preparation.

Contacts—The supraoccipital contacts the parietals dorsomedially and anteriorly, the prootic anteroventrally, the opisthotic posteroventrally, and there is a short contact with the exoccipital posterior to the suture with the opisthotic. The parietal-supraoccipital contact is long and anterodorsally convex in lateral view, curving ventrally along the anterior margin of the supraoccipital (Fig. 3B, G). In dorsal view, the sutures with the prootic and opisthotic are gently concave medially (Fig. 3E, J). These sutures meet in the lateral braincase wall at the prootic-opisthotic contact, precluding contact between the supraoccipital and quadrate. The contact with the exoccipital is approximately half the length of the contact with the opisthotic, and it is oriented in line with the posterior margin of the crista supraoccipitalis in lateral view.

Structures—The crista supraoccipitalis is tall, mediolaterally thin, and extends posterodorsally from the braincase to form much of the medial wall of each fossa temporalis superior. It is thickest along its posterior margin. In anterior view, the ventrolateral processes of the supraoccipital thicken ventrolaterally and are separated by a nearly right angle from one another ventrally (Fig. 3C, H). Thus, the supraoccipital forms approximately the dorsal half of the wall around the cavum cranii. The ventral-most tip of the left ventrolateral process within the cavum cranii is complete, forming a broad, nearly straight, anteroposteriorly oriented margin. This shows that the supraoccipital formed the dorsal margin of the hiatus acusticus, and lateral to it, the dorsal wall of the cavum labyrinthicum. Where this thin sheet of bone is broken away on the right ventrolateral process, the foramen aquaducti vestibuli can be seen in the posterodorsal corner of the cavum labyrinthicum.

Exoccipital

Preservation—The left exoccipital is preserved and mostly complete. The posterior tip of its contribution to the condylus occipitalis is worn, and the bone is missing its dorsal-most tip (which would articulate with the supraoccipital). It is also missing a fragment from its contact with the opisthotic dorsal to the foramen jugulare posterius and the ventrolateral corner of the bone that would have articulated along the posterior margin of the pterygoid.

Contacts—The exoccipital contacts the supraoccipital dorsally, the opisthotic anterolaterally, the pterygoid anteroventrally, and the basioccipital ventromedially. Its contact with the supraoccipital is very short and triangular in cross section. All other contacts between the exoccipital and other bones of the braincase are nearly straight in form and nearly equal in length.

Structures—The bone is roughly divided into dorsal and ventral halves by a series of structures through its middle. The dorsolateral corner of the bone, though incomplete, would have turned laterally to contact the opisthotic over the opening of the foramen jugulare posterius. This foramen is contiguous with the fenestra postotica, together seen as a single, large opening in posterior view (Fig. 3A, F). Medial to the foramen jugulare posterius, two small foramina are present in the middle of the concave posterior surface of the bone, the foramina nervi hypoglossi (Fig. 3A, F). The openings of these foramina within the cavum cranii are present on the medial wall of the bone, with the dorsal canal opening near the anteroposterior midpoint of this wall and the ventral canal opening anteroventral to it, just above the contact with the basioccipital (i.e., the basioccipital does not contribute to these foramina). A rounded ridge of bone projects perpendicularly (ventromedially) from the exoccipital-opisthotic suture dorsally over the foramina nervi hypoglossi to the condylus occipitalis. Although the tip of the condylus is incomplete, the preserved cross section of its base shows the unfused exoccipital-basioccipital suture, which demonstrates that each exoccipital would have formed roughly a 1/3 contribution to its dorsal extent (Fig. 3A, F). However, due to its incompleteness, it cannot be determined whether or not the exoccipitals

would have met along the dorsal edge of the condylus occipitalis. The exoccipital forms almost the entire lateral margin of the foramen magnum (Fig. 3A, F). In medial view, near its anterior end the bone forms the posterior border of the foramen jugulare anterius. This foramen is large and dorsoventrally tall, reaching half the height of the medial wall of the bone. It opens laterally into the recessus scalae tympani portion of the cavum acustico-jugulare, posterior to the processus interfenestralis of the opisthotic. The exoccipital forms the entire ventromedial wall of the recessus scalae tympani.

Basioccipital

Preservation—The basioccipital is mostly complete, only missing the posterior end of its contribution to the condylus occipitalis and the ventral tips of the tubercula basioccipitales.

Contacts—The basioccipital contacts the basisphenoid anteriorly, the pterygoid anterolaterally, and the exoccipital laterally and dorsolaterally. The contacts with the exoccipitals meet at the sagittal center of the base of the condylus occipitalis and descend ventrolaterally at nearly a right angle to one another, giving the bone an A shape in posterior view (Fig. 3A, F). In ventral view, the contact with the pterygoid is short and straight (as in most cryptodires; Gaffney 1979) (Fig. 3D, I), and the basioccipital-basisphenoid suture is posteriorly concave.

Structures—Though the tip of the condylus occipitialis is incomplete, its preserved base shows that the basioccipital would have formed the ventral 1/3 of the condyle (with the other 2/3 formed by the exoccipitals). A low, rounded, transverse ridge traverses the middle of the ventral face of the bone between the tubercula basioccipitales (Fig. 3D, I). This ridge divides the ventral surface into two halves: a posteroventrally facing, triangular depression posterior to the ridge and a shallowly bowled, ventrally-facing depression anterior to the ridge. The surface texture of both depressions is essentially smooth. Each tuberculum basioccipitale is rounded and, though ventrally incomplete, appears to have been formed almost entirely by the basioccipital (with essentially no contribution from the exoccipital). The dorsal surface of the basioccipital, forming the posterior end of the ventral floor of the cavum cranii, is triangular with a posterior point and shallowly concave. A low, posteriorly-pointed rise with a triangular, anterodorsal-facing surface is present at the sagittal midpoint of the suture with the basisphenoid; this structure forms the posterior half of the basis tuberculi basalis. The anterolateral margins of the dorsal surface rise to form dorsolaterally beveled ridges along the floor of the left and right hiatus acusticus.

Prootic

Preservation—Both prootics are missing their ventrolateral tip, including the majority of their contributions to each processus trochlearis oticum, but are otherwise mostly complete. The left prootic is additionally missing most of its anteroventromedial corner that would articulate with the basisphenoid.

Contacts—The prootic contacts the parietal anteriorly, the supraoccipital dorsomedially, the opisthotic posteriorly, the quadrate posterlaterally, the pterygoid ventrally, and the basisphenoid ventromedially. Contact with the basisphenoid is short and occurs along a dorsomedially-ventrolaterally beveled suture surface. The suture between the parietal and prootic is anteriorly convex in lateral view (Fig. 3B, G). The foramen stapedio-temporale bisects the medial portion of the suture to the quadrate.

Structures—Most of the processus trochlearis oticum is missing on both sides, but the left prootic preserves the medial portion of the processus. It occurs as a rounded, weakly keeled, anteroventrally facing ridge along the anterior border of the prootic (Fig. 3C, H). The prootic and quadrate contribute roughly equally to the border of the foramen stapedio-temporale in dorsal view (Fig. 3E, J), with the prootic forming the anteromedial half of the foramen and the medial wall of the canalis stapedio-temporalis and the aditus canalis stapedio-temporalis (its lateral opening). In posteroventral view, the anterodorsal corner of the cavum acustico-jugulare can be seen as a rounded cavity in the posterior face of the bone. Lateral to this corner, the prootic forms the dorsomedial margin of the foramen cavernosum. In medial view (from within the cavum cranii), the fossa acustico-facialis is positioned just anterior to the opening of the hiatus acusticus, dorsal to the contact with the basisphenoid. Within the fossa acustico-facialis, the foramen nervi facialis, occupied by the facial nerve in life (Gaffney 1979), is positioned ventral to a single opening for the foramen nervi acustici. The lateral exit of the foramen nervi facialis can be seen in the dorsomedial wall of the canalis cavernosus in ventrolateral view, the dorsal wall of which is formed by the prootic. The foramen nervi acustici exits laterally into the medial wall of the large cavum labyrinthicum. In oblique view through the foramen magnum, the recessus labyrinthicus prooticus portion of the cavum labyrinthicum can be seen to extend as a rounded space farther anteriorly than the cavum acustico-jugulare. The prootic also forms the anterior border of the fenestra ovalis (between the cavum labyrinthicum and the cavum

acustico-jugulare) and the posterodorsal border of the foramen nervi trigemini.

Opisthotic

Preservation—Both opisthotics are missing the posterolateral tip of the processus paraoccipitalis; the left opisthotic is otherwise complete. The right opisthotic is additionally missing the processus interfenestralis below the level of the foramen externum nervi glossopharyngei.

Contacts—As preserved, the opisthotic contacts the supraoccipital dorsomedially, the prootic anteriorly, the quadrate anterolaterally, and the exoccipital posteromedially; contact with the squamosal is uncertain due to the incompleteness of each processus paraoccipitalis. Contact with the quadrate is long, straight, and oriented anteromedially-posterolaterally in dorsal view (Fig. 3E, J). The contact with the prootic is shorter than the sutures with the supraoccipital and exoccipital.

Structures—The medial portion of the opisthotic hosts the recessus labyrinthicus opisthoticus portion of the cavum labyrinthicum, visible in anteromedial view through the hiatus acusticus as a deep, rounded pocket into the main body of the bone. In medial view, the processus interfenestralis extends slightly anteroventrally from the posterior wall of the cavum labyrinthicum to form the anterior wall of the foramen jugulare anterius and the recessus scalae tympani; it does not extend all the way to the basioccipital, indicating that the ventral portion of this wall would have been formed by cartilage in life. On the left side, the small foramen externum nervi glossopharyngei, visible through the fenestra postotica, passes mediolaterally through the processus interfenestralis to form the foramen internum nervi glossopharyngei in the ventral portion of the recessus labyrinthicus opisthoticus. The anterior margin of the processus interfenestralis forms the dorsal border of the fenestra ovalis, and the medial margin of the processus forms the lateral border of the fenestra perilymphatica (between the cavum labyrinthicum and recessus scalae tympani). The processus paraoccipitalis of the opisthotic, projecting posterolaterally from the main body of the bone, forms the dorsal roof of the cavum acustico-jugulare (Fig. 3A, F) and the recessus scalae tympani.

Basisphenoid

Preservation—The basisphenoid is complete except for the ventral surface of the bone and the majority of the anterior projection of the rostrum basisphenoidale.

Contacts—The basisiphenoid contacts the pterygoid ventrolaterally, the prootic dorsolaterally, and the basioccipital posteriorly. The contacts with the pterygoids face ventrolaterally, giving the bone a V shape in anterior view (Fig. 3C, H).

Structures—The size and shape of the ventral exposure of the basisphenoid are uncertain due to missing surface bone, but the texture of the sutures to the pterygoids and bone microstructure underlying what would have been the ventral surface appear to indicate it would have formed an anteriorly pointed triangle. The basisphenoid forms the anterior half of the basis tuberculi basalis at the dorsal midpoint of the suture with the basioccipital; this structure is well-developed (as in many cheloniids; Gaffney 1979) and comprised of a low, anteriorly-pointed rise with a triangular, posterodorsal facing surface (Fig. 3C, H). The majority of the dorsal surface of the bone, which forms the floor of the cavum cranii, is flat. However, the posterolateral margins of the dorsal surface rise to form laterally beveled shelves along the ventral margin of the left and right hiatus acusticus; these raised margins gradually heighten anteriorly. The flat dorsal surface ends anteriorly in the dorsum sellae, which is high relative to the sella turcica but not raised relative to the floor of the cavum cranii posterior to it. Though the anterolateral corners of the dorsum sellae are somewhat worn (Fig. 3C, H), the processus clinoideus appears to likely have been rounded and indistinct on each side, differing from most cheloniids (Brinkman et al. 2009) but similar to the poorly-developed condition in *Chelydra* (Gaffney 1979) and *Mexichelys coahuilaensis* Brinkman et al., 2009 (Brinkman et al. 2009). Posterior to the processus clinioideus on the right side, the posterior foramen nervi abducentis is preserved as a tiny opening, just below the contact with the prootic. Anterior to the dorsum sellae, the sella turcica is present as a deep, rounded depression that is posteriorly pointed in anterodorsal view (Fig. 3C, H). The paired foramen anterius canalis carotici cerebralis (faccc, which housed the internal carotids; Gaffney 1979) open ventrolaterally in the ventral floor of the sella turcica (Fig. 3C, H), and they are divided by a sagittal, keeled ridge of bone. The anterior foramen nervi abducentis is present as a tiny opening in the posterior border of each faccc. In ventral view, the canalis carotici cerebralis extends posteriorly and the canalis caroticus lateralis extends anteriorly from the faccc as shallow, similarly sized grooves in the ventrolateral face of the bone (Fig. 3D, I).

Dentary

Preservation—The left dentary is nearly complete, lacking only the dorsal portion of its contribution to the

processus coronoideus and its posteroventral-most projection that would suture to the floor of the surangular. This portion is also missing from the right dentary, but the base of the right surangular displays what the extent of this projection would have been. The right dentary is also missing its anterior-most tip.

Contacts—Before a crack running along the symphysis was glued during preparation, we observed that the contact would have been fused rather than sutured, as in most turtles (Gaffney 1979). The crack is sagittally aligned in dorsal view (Fig. 4A, D), but in ventral view the crack turns left laterally over its posterior half. Posteriorly, the dentary contacts the surangular, coronoid, angular, and prearticular. There is only a short contact with the anterior tip of the prearticular along the posteromedial wall of the foramen intermandibularis medius and floor of the sulcus cartilaginis meckelii (Fig. 4C, F). Sutural contact with the coronoid extends up to near the peak of the processus coronoideus. From this point, the dentary extends posteriorly to form a long, interdigitating contact with the surangular along the lateral face of the jaw (Fig. 4B, E). Though broken and missing, sutural contacts on the ventral aspect of the right surangular indicate a thin lip of the dentary would extend all the way to near the very posterior tip of the mandibular ramus. The dentary also has a long, straight sutural contact with the angular along the ventromedial edge of the mandibular ramus.

Structures—Only a slight dorsoventral thickening is seen along the dentary symphysis, primarily in the center of this contact. The lingual ridge is essentially nonexistent and the labial ridge is present as only a low lip along the external edge of the triturating surface. The triturating surface is overall slightly bowled. This surface is anteroposteriorly long, as in other taxa with an incipient or extensive secondary palate (e.g., *Erquelinnesia* Dollo, 1887 [Gaffney 1979]; *Pacifichelys hutchisoni* Lynch and Parham, 2003 [Parham and Pyenson 2010]), and it is distinctly broader at the symphysis than near the coronoid, forming a clearly triangular beak in dorsal view (Fig. 4A, D). Foramina-rich bone indicates that the rhamphotheca (keratinous beak) would have ended just anterior of the processus coronoideus, and would have cut across the lateral aspect of the dentaries just anterior to the foramen dentofaciale majus. A shallow furrow running transversely along the ventral aspect of the dentaries defines the break between foramina-rich bone anteriorly and smooth bone posteriorly, hence defining the posterior margin of the rhamphotheca. A shallow fossa on the lateral face extends from behind the foramen dentofaciale majus to the lateral tip of the surangular (Fig. 4B). A narrow ridge along the ventrolateral edge of the dentary defines the bottom of this depression, which would have served as an attachment region for the external jaw adductors (Gaffney 1979). The sulcus cartilaginis meckelii runs along the medial aspect of the dentaries and continues without interruption across the symphysis. Where the sulcus enters the fossa meckelii (via the foramen intermandibularis medius), the foramen alveolare inferius is present as a small opening in its dorsolateral wall.

Angular

Preservation—The right angular is complete except for its posterior tip, but the left angular is missing its anterior half, posterior tip, and a portion of its ventromedial face.

Contacts—The angular forms the ventromedial edge of most of the mandibular ramus, abutting against the ventral edge of the prearticular for its entire length (Fig. 4C, F). It sutures laterally to the dentary and comes to a distinct point at both anterior and posterior ends, beneath the prearticular and articular, respectively. By removing the unfused right articular and viewing inside the fossa meckelii, the angular can be seen to have a long, dorsolateral sutural contact with the surangular.

Structures—The angular is an elongate element that comes to a distinct tip at its anterior end. It is the primary element forming the floor of the fossa meckelii. Much of the dorsal surface of the posterior end of the angular abuts against the bottom of the articular (Fig. 4C). The foramen intermandibularis caudalis passes obliquely through the angular-prearticular suture near its midpoint on the medial face of the mandibular ramus (Fig. 4F). The posterior end of each angular is too incomplete to allow delineation of either foramen for the chorda tympani.

Surangular

Preservation—The right surangular is complete, but most of the left surangular is missing. Only the anterior and ventral portions of the left surangular remain along its suture with the left dentary (Fig. 4A).

Contacts—A vertical suture to the posterior edge of the dentary can be seen within the fossa meckelii, descending just behind the processus coronoideus. In lateral view, the suture with the dentary runs posteroventrally back from the processus coronoideus (Fig. 4B, E). This suture takes a small, sigmoid step anteriorly near the ventral edge of the jaw. Only a very short suture with the coronoid occurs just posterior to the processus coronoideus (Fig. 4A, D). The entire ventromedial edge of the surangular shares

a suture with the angular. Medially, the surangular abuts against the anterior process of the articular.

Structures—The foramen nervi auriculotemporalis is present just posterodorsal to the dentary suture on the lateral face of the surangular (Fig. 4B, E). It is located within the small anterior embayment of the suture to the dentary and passes anteromedially through the surangular into the lateral wall of the fossa meckelii. A thin wall of bone projects off the medial face of the surangular to enshroud part of this foramen within the fossa meckelii; this wall is visible as a curved lip in dorsal view (Fig. 4A, D). Most of the dorsal surface of the surangular is flat, despite it making no contribution to the area articularis mandibularis (jaw joint). The lateral wall of the fossa meckelii (formed by the surangular) extends higher than the medial wall (formed by the prearticular) (Fig. 4C, F). The posterior half of the surangular curves medially and tapers to a point that terminates posteriorly into a small lateral pocket of the articular (Fig. 4A, D). Unlike living cheloniids (Gaffney 1979), there is no contribution from the surangular to the area articularis mandibularis.

Coronoid

Preservation—The right coronoid is complete but only the ventral half of the left coronoid is preserved.

Contacts—The coronoid contacts the dentary, prearticular, and surangular. Its entire anterior edge contacts the posterodorsal edge of the dentary, and this slope descends anteroventromedially from the high processus coronoideus (Fig. 4C, F). Posterolaterally to the peak of the processus coronoideus, the coronoid has a short suture with the anterior end of the surangular (Fig. 4A, D). A long suture surface unites the coronoid with the prearticular on the medial surface of the mandibular ramus (Fig. 4C, F). This surface is roughly half as long as the suture of the coronoid with the dentary.

Structures—The coronoid forms the peak of the processus coronoideus. Its ventralmost border forms the dorsal margin of the foramen intermandibularis medius. The coronoid also forms the anterior margin of the fossa meckelii and encloses the dorsal border of the space connecting this fossa to the sulcus cartilaginis meckelii (Fig. 4C, F).

Articular

Preservation—The right articular is complete and is preserved as an unfused element that can be removed from the posterior end of the jaw. Only the ventral portion of the anterior projection (that articulates between the surangular and prearticular) of the left articular is preserved (Fig. 4D).

Contacts—The anterior process of the right articular forms the posterodorsal wall of the fossa meckelii (Fig. 4A, D). The ventral border of this process lies against the dorsal margin of the posterior third of the angular. Striations for fusion with the prearticular are located on the ventral side of the medial area articularis mandibularis facet and along the ventromedial edge of the anterior process.

Structures—The right articular is complex in form, with a somewhat backwards "L" shape in dorsal view (Fig. 4A, D). Its anterior process exhibits a deep conical depression in the anterior face, pointing directly into the fossa meckelii. In anterior view the process is subquadrangular in form with a flat dorsal margin, and it tapers in dorsoventral thickness posteriorly. It occupies half of the element in dorsal view. The other half of the element in dorsal view forms the area articularis mandibularis, which is divided into equidimensional medial and lateral facets (Fig. 4A, D). The medial facet is tilted generally anterolaterally while the lateral facet is canted posteroventrally. A thin ridge extends from the medial edge of the anterior process towards the medial facet, and the medial facet is quite thin dorsoventrally. There is no processus retroarticularis; this is the expected condition in cheloniids (Lehman and Tomlinson 2004).

Prearticular

Preservation—The right prearticular is mostly complete, only lacking its posterior third (Fig. 4C); this portion of the left prearticular is almost entirely preserved (only the posterodorsal-most corner is not present). Most of the dorsal extent of the left prearticular is also missing, as is its anterior tip.

Contacts—The right prearticular contacts the dorsomedial surface of the angular for most of its length (Fig. 4C, F). Only at its very thinly tapered anterior end does it suture to the dentary, forming part of the floor and medial wall of the foramen intermandibularis medius. A thin span sutures anterodorsally to the coronoid. The posterodorsal end of the left prearticular twists medially, creating a dorsolateral contact with the articular.

Structures—The prearticular forms nearly the entire medial wall of the mandibular ramus, thereby also forming the medial wall of the fossa meckelii (Fig. 4A, D). Thickness of the prearticular slightly increases posteriorly as the element gains robustness to form a ventromedial contact with the articular. It does not appear to contribute to the floor of the fossa meckelii, but its anterior-most tip forms a small portion of the floor

of the sulcus cartilaginis meckelii. The small foramen intermandibularis caudalis bisects the suture to the angular near its anteroposterior midpoint (Fig. 2F). There is no indication of the foramen intermandibularis oralis on either side. Incompleteness of the posterodorsal margin of each prearticular prevents determination of whether or not the canalis chorda tympani mandibularis passed through the prearticular or along the prearticular-articular suture, if it was present at all.

DISCUSSION

Taxonomic identity of RU-EFP-00009

As noted by Parham (2005), remains of diverse turtle species are commonly found in close association in the MFL, having in the past led to misidentification and mixed (chimeric) specimens. In this case, the skull and mandible of RU-EFP-00009 were originally presumed to belong to a similarly-sized individual of the pleurodire *Taphrosphys sulcatus* (RU-EFP-00001, comprised of a partial plastron, carapace, and postcranial remains) found adjacent to them in the MFL (Ullmann and Lacovara 2011). However, the presence of multiple chelonioid and pan-cheloniid synapomorphies identifies the skull and mandible as instead belonging to a pan-cheloniid. Specifically, RU-EFP-00009 exhibits the following chelonioid synapomorphies (thus differentiating it from pleurodires such as *Taphrosphys*): (1) squamosal-quadrate contact wide open (**39:1**); (2) posterior surface of the opisthotic paraoccipital process dorsoventrally convex (**132**:**2**); (3) dorsum sellae high (Gaffney 1975, Hirayama 1998, Evers and Benson 2018 [**139**:**2**]); (4) paired foramina anterius canalis carotici cerebralis lie close together (Gaffney 1975, Hirayama 1998, Evers and Benson 2018 [**142**:**1**]); (5) basis tuberculi basalis developed on the basisphenoid in addition to the basioccipital (**144**:**1**); and (6) foramen jugulare posterius coalescent with the fenestra postotica (**163:1**). Within this clade, RU-EFP-00009 can be assigned to a pan-cheloniid based on its dorsolaterally-directed orbits (Hirayama 1998) and a rod-like rostrum basisphenoidale (Parham 2005, Myers et al. 2017). RU-EFP-00009 exhibits only one of five unambiguous synapomorphies for total-group Cheloniidae identified by Evers and Benson (2018), large foramen dentofaciale majus in the dentary (**176:1**), indicating it is best assigned to a pan-cheloniid turtle.

Gallagher (1993, 2003) previously reported three pan-cheloniid taxa from the MFL of the Hornerstown Formation, *Catapleura repanda* Cope, 1868b (as *Dollochelys atlantica* Zangerl, 1953), *Peritresius ornatus* Baird, 1964 (as *P.* cf. *emarginatus* Leidy, 1856), and *Euclastes wielandi* (as *Osteopygis emarginatus* Cope, 1867). The skull of *C. repanda* remains unknown, and the only overlapping element between *P.* ornatus and RU-EFP-00009 is the dentary. The dentary of RU-EFP-00009 differs from the dentary of *P. ornatus* (based on personal observations by PVU and ZMB of NJSM 11051, described by Baird [1964]) by having: (1) the foramen dentofaciale majus present (it is absent in NJSM 11051); and (2) a shallow fossa in the lateral face of the dentary posterior to this foramen, whereas in *Peritresius* this region is convex (Baird 1964, fig. 1B). As observed in RU-EFP-00009, an elongate, wide, flat mandibular triturating surface and a broadly rounded anterior border to the mandible are each considered autapomorphic of *Euclastes* (Lynch and Parham 2003, Weems and Brown 2017). We therefore assign RU-EFP-00009 to the genus *Euclastes*. Among the three currently valid species of *Euclastes* (*Eu. wielandi*, *Eu. acutirostris*, and *Eu. platyops* Cope, 1867), symphyseal swelling in the mandibular triturating surface (usually, but not always, present; see Zangerl 1953) is considered autapomorphic of *Eu. wielandi* (Hirayama and Tong 2003), and presence of the foramen dentofaciale majus and a lateral fossa in the dentary are also characters known in *Euclastes wielandi* (personal observation of NJSM NH 2006.7 by PVU and ZMB; AMNH 30030, Hirayama and Tong 2003). This identification is further supported by a combination of chelonioid traits in the skull present in the NJSM 11872 specimen of *Eu. wielandi*: dorsum sellae and processus clinoideus only moderate in height (Fastovsky 1985), and dorsally-directed orbits within a very low and wide skull (Fastovsky 1985, Parham 2005). Finally, prior discovery of other specimens confidently attributed to *Eu. wielandi* (e.g., NJSM 11872; Fastovsky 1985) from the same horizon (the MFL) at the same locality (Edelman Fossil Park, formerly the Inversand Company mine) further supports identification of RU-EFP-00009 to *Eu. wielandi*.

Based on its size being only about two-thirds that of NJSM 11872, we infer RU-EFP-00009 was a subadult. Lack of fusion of sutures within the condylus occipitalis and the skull roof showing only incipient fusion of the right prefrontal-frontal suture in RU-EFP-00009 further support its identification as a subadult and exclude many differences between RU-EFP-00009 and other specimens of *Eu. wielandi* being attributable to sexual dimorphism. As in most vertebrates, sutures between the skull roof elements and within the condylus occipitalis are known to fuse with age in turtles (Hay 1908, Gaffney 1979, Hirayama 1985, Matzke 2007). Though RU-EFP-00009

consists of only cranial and mandibular remains, histology could also be a fruitful endeavor in the future to further test the ontogenetic age of this turtle.

Taphonomic interpretations

The isolated nature of the skull and mandible of RU-EFP-00009 is suggestive of deposition on the sea floor via detachment from a "bloat-and-float" carcass (Schwimmer 1997, Boles 2016). Once on the sea floor, we infer that the skeletal remains were buried rapidly because of their generally well-preserved and largely articulated state despite lack of fusion among cranial and mandibular elements. Absence of evidence for invertebrate grazing and vertebrate scavenging further support rapid burial of RU-EFP-00009 (cf., Boles 2016). However, because the skull roof was discovered ventral side up with the palatal portion of the skull missing, burial was likely only partial (i.e., deposition of a few centimeters of sediment would be enough to bury the skull roof and braincase but not the palatal portion of the skull). As with other skeletons from the MFL (Boles 2016) vertebrate and invertebrate scavengers may have aided any weak currents in moving the braincase to its final, disarticulated position relative to the skull roof.

Although discerning the origin of the MFL was well beyond the scope of this study, we note that RU-EFP-00009 is one of many subadult marine reptiles known from the MFL. Juvenile and subadult turtles and crocodilians are a common occurrence in this bonebed. Examples which we are aware of, most of which are as yet unpublished, include the fused dentaries of a subadult *Eu. wielandi* (NJSM 13887), cranial and shell material of a subadult *Bothremys* sp. (RU-EFP-00003), partial juvenile carapaces of a *Peritresius ornatus* (RU-EFP-00017) and a *Taphrosphys sulcatus* (RU-EFP-00027), a partial skull of a subadult *Ta. sulcatus* (NJSM 11362), a partial skull of a subadult (marine crocodile) *Hyposaurus rogersii* Owen, 1849 (RU-EFP-00007, provisionally described in a conference abstract by Carter et al. 2012), craniomandibular remains of a juvenile (marine crocodile) *Thoracosaurus neocesariensis* De Kay, 1842 (RU-EFP-00022), and cranial and postcranial remains of a subadult *Th. neocesariensis* (RU-EFP-00006, provisionally described in a conference abstract by Voegele et al. 2011). Given the decades of collecting at this site (Ullmann et al., in press), remains of additional subadult individuals are undoubtedly present in the collections of the Academy of Natural Sciences, the New Jersey State Museum, and the American Museum of Natural History. Although some of these specimens fall within the possible range of sexual dimorphism in adult body sizes, most clearly pertain to subadults based on either histology, osteologic features, and/or distinctly small size (in other words, a size difference among specimens beyond that known to be possible for sexual dimorphism in extant turtles [~17%; Ceballos et al. 2013] and crocodilians [~20%; Warner et al. 2016 and references therein]). Taphonomically, the abundance of subadults in addition to adult individuals in the MFL may be suggestive of an event causing widespread ecosystem disruption and thus mass death rather than protracted, attritional accumulation of carcasses (Boles 2016). We infer this because mass death assemblages are commonly characterized by nonselective mortality and thus a relatively even distribution of individuals of all age classes rather than a skewed distribution towards only juveniles or adults (Varricchio and Horner 1993, Turnbull and Martill 1988, Lauters et al. 2008). Further, Esmeray-Senlet et al. (2017) reported the discovery of an iridium anomaly within the MFL, which supports the proposition by Gallagher (1993, Gallagher et al. 2011) that the MFL may represent "immediate post-[Chicxulub] impact mortality in the wake of deteriorating environmental conditions after bolide impact". Taphonomic and geochemical analyses are currently underway to further test this hypothesis.

Phylogenetic insights

Study of RU-EFP-00009 and our personal observations of the complete skull of NJSM 11872 revealed anatomical insights relevant to phylogenetic studies of *Euclastes* and Chelonioidea. In particular, these specimens permit coding of six phylogenetic characters which were previously unknown in the most recent derivative of the Cadena and Parham (2015) matrix by Evers and Benson (2018). These new character scorings are as follows: basisphenoid, dorsum sellae high, (**139:2**); basisphenoid, foramina anterius canalis carotici cerebralis close together in anterodorsal view, (**142:1**); foramen jugulare posterius, coalescent with fenestra postotica, (**163:1**); cranial scutes, scute X much smaller than scute D, (**167:1**); cranial scutes, scute X partially separates scutes G, (**168:1**); dentary-surangular arrangement, posterior expansion of dentary present and covering the dorsal half of the surangular in lateral view, surangular with anterior projection, (**177:1**). A phylogenetic analysis was outside the scope of this study because of the low sample size of *Euclastes* specimens and our focus on intraspecific variation rather than interspecific relationships, but the above character scorings provide valuable additions to existing phylogenetic matrices (e.g., Cadena and Parham

2015). Our comparative studies also revealed patterns of intraspecific variation among specimens of *Eu. wielandi* (discussed in the next section) related to two other characters, **10** and **85**, in the Cadena and Parham (2015) matrix, signifying that these two characters should be disused in future derivations of this matrix.

Intraspecific variation in *Euclastes wielandi*

Although considerable work has been done to examine bilateral asymmetry, sexual dimorphism, and ontogenetic, individual, and ecomorphological variation in turtle shell morphology (Hay 1908, Zangerl 1953, 1969, 1980, Fichter 1969, Brinkman and Nicholls 1991, Rivera 2008, Gilbert et al. 2001, Reynoso and Montellano-Ballesteros 2004, Tong et al. 2006, Scheyer et al. 2008, Ceballos et al. 2013, Ferreira et al. 2016), such variations within the skull, and especially the mandible, have received less attention. To date, studies examining intraspecific variation in cranial morphology have primarily focused on individual taxa (e.g., Dalrymple 1977, Lindeman 2000, Sánchez-Villagra and Winkler 2006, Matzke 2007, 2008, Bever 2009a, b, Lyson and Joyce 2009, but see Joyce and Bell 2004 for a broader study), and a large-scale comparative analysis of cranial ontogeny in recent and fossil turtles is still lacking. Although such a comprehensive review is beyond the scope of this work, we note a few commonalities in the above reports of relevance to RU-EFP-00009, with particular emphasis on two studies of juvenile pan-chelonioids (*Ctenochelys* and *Toxochelys* Cope, 1873) by Matzke (2007, 2008).

The basioccipital is dorsally exposed in the condylus occipitalis in juveniles of *Ctenochelys* (Matzke 2007) and the extant turtles *Lepidochelys* Fitzinger, 1843 and *Chelonia* (Zangerl 1953); through growth in these taxa, the exoccipitals expand dorsally over the basioccipital within the condylus. Since the exoccipitals dorsally cover the basioccipital in RU-EFP-00009 as well as adult individuals of *Euclastes wielandi* (e.g., NJSM 11872), it appears that either: (1) *Eu. wielandi* does not share this ontogenetic trend; or (2) the exoccipitals expand over the basioccipital earlier in ontogeny in *Euclastes* (i.e., the basioccipital would be dorsally exposed in individuals younger than RU-EFP-00009). Also in contrast to *Ctenochelys* (Matzke 2007), a canal formed by the facial nerve is clearly present in the prootic and the sella turcica is positioned close to the dorsum sellae in both RU-EFP-00009 (Fig. 3C, H) and adults of *Eu. wielandi* (e.g., NJSM 11872), rather than closer to it in subadults. Nonetheless, until the discovery of *Eu. wielandi* individuals younger than RU-EFP-00009, it remains unclear if these conditions would be similar between the two taxa in young juveniles.

Matzke (2008) found that the processus trochlearis oticum changes from anteriorly concave to straight or convex through ontogeny in the pan-chelonioid *Toxochelys*. Although the processus trochlearis oticum is slightly less robust in RU-EFP-00009 than in NJSM 11872 (personal observation by PVU and ZMB), it is present as a convex ridge in the former specimen (Fig. 3C, H). However, because it is unknown if RU-EFP-00009 and specimen USNM 12009 of *Toxochelys* represent individuals of similar ontogenetic age, it remains uncertain whether *Euclastes* and *Toxochelys* do not share this ontogenetic trend or if the processus reached "adult" form earlier in ontogeny in *Euclastes* than in *Toxochelys*.

Prior comparative studies have also found ontogenetic and intraspecific variation in cranial and mandibular morphology specifically in *Eu. wielandi*. Zangerl (1953) noted that development of symphyseal swelling in the triturating surface of the mandible varies among specimens, and we have also observed this among *Eu. wielandi* specimens at the New Jersey State Museum. Zangerl (1953) and Hirayama and Tong (2003) also found variation in the anteroposterior length of the triturating surface in mandibles of *Eu. wielandi*, and we have observed that this is associated with body size (longer triturating surface in larger individuals; personal observation of NJSM specimens by PVU and ZMB). The secondary palate and mandibular triturating surface are also known to expand through growth in *Ctenochelys* (Matzke 2007), *Pseudemys texana* Baur, 1893 (Bever 2009b), *Sternotherus odoratus* Latreille, 1801 (Bever 2009a), and modern carettines (Bjorndal 1997), demonstrating that an adaptive shift through ontogeny toward increased durophagy (similar to that observed in extant *Apalone ferox* Schneider, 1783; Dalrymple 1977) is a common growth trajectory among cryptodirans. Parham et al. (2014) further noted that the tomial ridge on the upper palate varies in height among specimens of *Eu. wielandi*, and the pan-cheloniid *Pacifichelys urbinai* Parham and Pyenson, 2010 also exhibits variation in tomial ridge height (Parham and Pyenson 2010). Finally, Hirayama and Tong (2003) identified variation in the relative development of the secondary palate among skulls of *Eu. wielandi*, specifically in the anteroposterior length of the vomer and vomerine pillar. In general, most of these intraspecific variations are associated with the morphology of the feeding apparatus, suggesting slight changes in diet through ontogeny and potential individual variation in feeding ecology (as in extant *Apalone* [Dalrymple 1977], *Sternotherus* [Bever 2009a], *Pseudemys* [Bever 2009b],

and carettines [Bjorndal 1997, Ramirez et al. 2015]). Phylogenetically, these features are therefore also likely subject to functional homoplasy (Jalil et al. 2009, Parham and Pyenson 2010).

Our comparisons of RU-EFP-00009 to other complete skulls and mandibles of *Eu. wielandi* (NJSM 11872 [Fastovsky 1985], AMNH 30022 [Hirayama and Tong 2003], IGPS 590/1 [Karl et al. 1998]) revealed additional, previously unreported, variations in cranial morphology related to ontogeny and individual variation. The most striking difference between RU-EFP-00009 and other specimens of *Eu. wielandi* is the very small contribution of the frontal to the margin of the orbit in RU-EFP-00009 (Figs. 2, 5). While similar to the condition in *Eu. acutirostris* (Jalil et al. 2009), as shown in Figure 5, this morphology starkly contrasts the wide contribution of the frontal to the orbit in other *Eu. wielandi* specimens (NJSM 11872 and AMNH 30022; Fastovsky 1985, Hirayama and Tong 2003). Additionally, because the sulcus between the prefrontal and supraorbital scales is geometrically in the same general position as in the larger specimens, the difference in the underlying bone architecture causes the scale sulcus to traverse over the posterolateral projection of the prefrontal, adjacent to the orbit (Fig. 2D). This condition again differs from NJSM 11872 (personal observation by PVU and ZMB) and AMNH 30022 (Hirayama and Tong 2003, fig. 3), in which the sulcus solely traverses the frontal (Fig. 5). Clearly, these two features are associated. It is unlikely that these differences are due to ontogeny because the skull of RU-EFP-00009, though smaller than that of NJSM 11872, is roughly the same size as that of AMNH 30022. Therefore, frontal retraction and the precise course of the prefrontal-subraorbital scale sulcus appear to be more likely subject to individual variation. In other turtles, relative retraction of the frontal from the orbit is known to vary among individuals in *Chelonia mydas* (Gaffney 1979) and multiple testudinoids (Joyce and Bell 2004) and emydids (Gaffney 1979, Stephens and Wiens 2003), as well as ontogenetically in *Ctenochelys stenoporus* (Matzke 2007) and bilaterally in one specimen each of *Ch. mydas* (Tong and Hirayama 2008) and *Pseudemys texana* (Bever 2009b). These variations are significant because frontal retraction has historically been used as a feature of taxonomic significance (e.g., in the diagnosis of *Argillochelys africana*; Tong and Hirayama 2008) and as a character in phylogenetic analyses (e.g., **4** of Hirayama [1994]; **3** of Joyce and Bell [2004]; **10** of Cadena and Parham [2015]; **11** of Evers and Benson [2018]). Demonstration that this feature is subject to individual, bilateral, and ontogenetic variation in extant and fossil chelonioids signifies this is a poor trait for use in taxonomic diagnoses and phylogenetic analyses.

Two other differences we found between RU-EFP-00009 and other specimens of *Eu. wielandi* appear to reflect variation in the extent of ossification due to ontogeny. First, whereas in RU-EFP-00009 the anterior projection of the articular is short and leaves a gap between the prearticular and surangular, in the larger mandible of NJSM NH 2006.7 the anterior projection of the articular is elongate, extending forward to form a triangular point filling the posterior region of the fossa meckelii and leaving no gap between the prearticular and surangular. We infer that the anterior gap in RU-EFP-00009 was likely occupied by cartilage in life because the articular is known to be cartilaginous in an extant turtle (*Dermochelys* Blainville, 1816) and because the articular is the only bone in the lower jaw of turtles that ossifies from cartilage (Gaffney 1979). Matzke (2007) similarly inferred that the articular may have been at least partially formed by cartilage in juveniles of *Ctenochelys*. Second, whereas the processus interfenestralis of the opisthotic extends to the floor of the cavum acustico-jugulare in the large skull of NJSM 11872, in the smaller specimen RU-EFP-00009 the process is thin and does not reach the floor of the cavum, implying that its ventral end was formed by cartilage. Variations in the length and robustness of the processus interfenestralis have been used as character states in phylogenetic analyses (e.g., **85** of Cadena and Parham [2015] and all more recent studies using that matrix). However, this process is known to progressively ossify from cartilage through ontogeny in some turtles (e.g., *Sternotherus odoratus*; Bever 2009a). That the morphology of this process changes through ontogeny signifies care should be taken to ensure use of only definitive "adult" specimens when using this character in phylogenetic studies.

Finally, four additional differences were also identified between NJSM 11872, NJSM 16811, and RU-EFP-00009. First, whereas in NJSM 11872 the foramina nervi hypoglossi originate within the basioccipital in the cavum cranii (Fastovsky 1985), in RU-EFP-00009 their entrances are fully within the exoccipital. Second, the precolumellar fossa is apparent as a small, conical cavity in RU-EFP-00009 (Fig. 3B, G), but it is indistinct in NJSM 11872 and NJSM 16811 (personal oservation by PVU and ZMB). Third, the bar between the faccc in RU-EFP-00009 exhibits a sharp dorsal keel whereas this bar is wider and flatter in NJSM 11872. Bever (2009b) observed individual variation in the width of this bar in *Pseudemys texana*. Fourth, in RU-EFP-00009 the basisphenoid appears

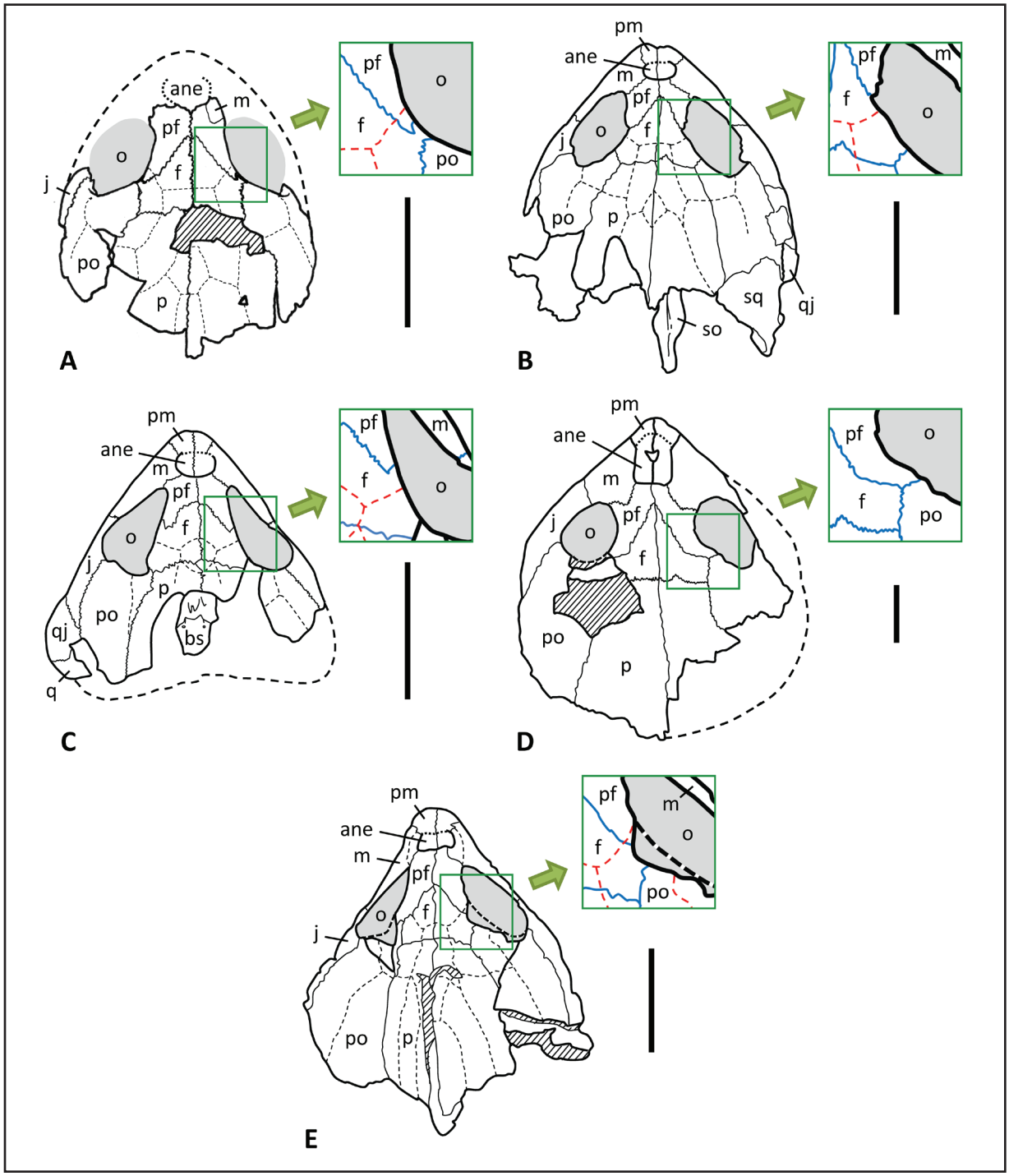

Figure 5. Comparison of the skulls of the three currently valid species of *Euclastes* in dorsal view, highlighting variation in the contribution of the frontal to the orbital rim and the path of the prefrontal-subraorbital scale sulcus. Specimens scaled to approximately the same anteroposterior length. In each primary figure, cranial bone sutures are shown as solid lines and scale sulci are shown as dashed lines. In each inset, sutures between bones are shown as blue lines and cranial scale sulci are shown as red dashed lines. (**A**) *Euclastes wielandi*, subadult specimen RU-EFP-00009. (**B**) *Euclastes wielandi*, adult specimen NJSM 11872 (redrawn after Fastovsky 1985, fig. 2). (**C**) *Euclastes wielandi*, adult specimen AMNH 30022 (redrawn after Hirayama and Tong 2003, fig. 3A). (**D**) *Euclastes platyops*, holotype specimen ANSP 10187 (redrawn after Hay 1908, plate 29 fig. 2). No scale sulci are shown because personal observation of this specimen (by PVU) confirmed that no sulci are present on the dorsal surface of the skull. (**E**) *Euclastes acutirostris*, holotype specimen OCP.DEK/GE 408 (redrawn after Jalil et al. 2009, fig. 3A). **Abbreviations**: **ane**, apertura narium externa; **bs**, basisphenoid; **f**, frontal; **j**, jugal; **m**, maxilla; **o**, orbit; **p**, parietal; **pf**, prefrontal; **pm**, premaxilla; **po**, postorbital; **q**, quadrate; **qj**, quadratojugal; **so**, supraoccipital; **sq**, squamosal. Hashing indicates broken, missing, and/or eroded surfaces. Scale bars=5 cm.

strongly V-shaped in anterior view and has a rounded sella turcica, but in NJSM 16811 the basisphenoid is dorsoventrally flatter in anterior view, forming a broader, shallower V, and the sella turcica is shallower. We refrain from assigning these intraspecific variations specifically to ontogeny, sexual dimorphism, or individual variation given the low sample size and inability to determine the gender of the individuals.

CONCLUSIONS

Although the most common discoveries of large vertebrates in Cretaceous–Paleogene marine sediments of the Atlantic Coastal Plain are of turtles, the majority of these taxa remain poorly characterized due to the fragmentary nature of their fossil record. A new specimen recently recovered from the Main Fossiliferous Layer of the Hornerstown Formation at the Jean and Ric Edelman Fossil Park at Rowan University, consisting of a subadult skull and mandible of the pan-cheloniid *Euclastes wielandi* (RU-EFP-00009), provides valuable insights into the anatomy and intraspecific variation in morphology of this historically important taxon. Our study of RU-EFP-00009 and others of *Eu. wielandi* at the New Jersey State Museum revealed new phylogenetic character scorings for this taxon of characters in common use in recent cladistic analyses (e.g., Cadena and Parham 2015, Gentry et al. 2018), including the presence of a high dorsum sellae on the basisphenoid, coalescent fenestra postotica and foramen jugulare posterius, sigmoid dentary-surangular suture on the lateral face of the mandible, and other attributes. These phylogenetic insights should be employed in future cladistic analyses.

Euclastes wielandi exhibits moderate expansion of the mandibular triturating surface indicative of a shift in feeding ecology through ontogeny towards a more durophagous diet. Similar proportional expansion of the secondary palate and mandibular triturating surface in *Ctenochelys* (Matzke 2007), *Pseudemys* (Bever 2009b), *Sternotherus* (Bever 2009a), and modern carettines demonstrates that ontogenetic progression towards increased durophagy is a common life history trait/adaptation within Cryptodira.

Lastly, RU-EFP-00009 exhibits a uniquely small contribution of the frontal to the orbital margin and a unique path for the prefrontal-supraorbital scale sulcus compared to other specimens of *Eu. wielandi*. Review of prior reports on variation in frontal retraction among fossil and extant turtles revealed that the morphology of this bone and therefore also the scale sulcus crossing its dorsal surface is subject to considerable intraspecific variation in diverse cryptodirans via bilateral asymmetry, individual variation, and ontogeny. Because of this clear morphologic plasticity in the frontal and its contributions to the surrounding skull roof features, we recommend that extreme caution be taken in any future use of the morphology of this bone in taxon diagnoses or phylogenetic analyses.

ACKNOWLEDGEMENTS

In 2010, Inversand Mining Company graciously allowed site access and collection of specimens from their open pit mine and assisted in overburden removal. Much thanks is owed to the company and its employees for their assistance in the field and support of vertebrate paleontology. Gratitude is also extended to R. Pellegrini and D. Parris of the New Jersey State Museum and N. Gilmore of the Academy of Natural Sciences of Drexel University for opening their collections for comparative studies. Special thanks are given to E. Gaffney for providing us with insight, suggestions, lunch, and some good stories early on in this study. We further thank Jean and Ric Edelman for their generous support of the Fossil Park bearing their names, and Rowan University and Mantua Township for their dedication to preserving the site in perpetuity and continued support of earth science and STEM education in southern New Jersey. Comments from J. Parham, E. Cadena, and D. Lawver greatly improved the manuscript. This work was supported by Drexel University, Southern Connecticut State University, and Rowan University.

LITERATURE CITED

Bailleul, A.M., J.B. Scannella, J.R. Horner, and D.C. Evans. 2016. Fusion patterns in the skulls of modern archosaurs reveal that sutures are ambiguous maturity indicators for the Dinosauria. *PLoS ONE* 11:e0147687.

Baird, D. 1964. A fossil sea-turtle from New Jersey. *New Jersey State Museum Investigations* 1:1–26.

Batsch, A.J. 1788. Versucheiner Anleitung, zur Kenntiniß und Geschichte der Tiere und Mineralien. Akademische Buchhandlung, Jena. 528 pp.

Baur, G. 1893. Notes on the classification of the Cryptodira. *American Naturalist* 27:672–674.

Bever, G.S. 2009a. Postnatal ontogeny of the skull in the extant North American turtle *Sternotherus odoratus* (Cryptodira: Kinosternidae). *Bulletin of the American Museum of Natural History* 330:1–97.

Bever, G.S. 2009b. The postnatal skull of the extant North American turtle *Pseudemys texana* (Cryptodira: Emydidae), with comments on the study of discrete intraspecific variation. *Journal of Morphology* 270:97–128.

Bjorndal, K.A. 1997. Foraging ecology and nutrition of sea turtles. Pp. 199–231 *in* Lutz, P.L. and Musick, J.A. (eds.). The biology of

sea turtles. CRC Press, Boca Raton.
Blainville, H.M. 1816. Prodrome d'une nouvelle distribution systématique de règne animal: reptiles. *Bulletin de la Société Philomathique de Paris* 111:119.
Boles, Z.M. 2016. Vertebrate taphonomy and paleoecology of a Cretaceous-Paleogene marine bonebed. Ph.D. diss. Drexel University, Philadelphia, PA.
Brinkman, D.B., and E.L. Nicholls. 1991. Anatomy and relationships of the turtle *Boremys pulchra* (Testudines: Baenidae). *Journal of Vertebrate Paleontology* 11:302–315.
Brinkman, D.B., M.C. Aquillon-Martinez, C.A. Dávila, H. Jamniczky, D.A. Eberth, and M. Colbert. 2009. *Euclastes coahuilaensis* sp. nov., a basal cheloniid turtle from the Late Campanian Cerro del Pueblo Formation of Coahuila State, Mexico. *PaleoBios* 28:76–88.
Cadena, E.A., and J.F. Parham. 2015. Oldest known marine turtle? A new protostegid from the Lower Cretaceous of Colombia. *PaleoBios* 32:1–42.
Carter, A.M., Z.M. Boles, E.R. Schroeter, and K.J. Lacovara. 2012. A juvenile *Hyposaurus rogersii* skull from the Hornerstown Formation of New Jersey. *Journal of Vertebrate Paleontology* 32(Supp):75A.
Ceballos, C.P., D.C. Adams, J.B. Iverson, and N. Valenzuela. 2013. Phylogenetic patterns of sexual size dimorphism in turtles and their implications for Rensch's Rule. *Evolutionary Biology* 40:194–208.
Cope, E.D. 1867. On *Euclastes*, a genus of extinct Cheloniidae. *Proceedings of the Academy of Natural Sciences of Philadelphia* 19:39–42.
Cope, E.D. 1868a. On the origin of genera. *Proceedings of the Academy of Natural Sciences of Philadelphia* 20:242–300.
Cope, E.D. 1868b. A new species of *Chelonia* from New Jersey. *Proceedings of the Academy of Natural Sciences of Philadelphia* 20:147.
Cope, E.D. 1873. Description of *Toxochelys latiremis*. *Proceedings of the Academy of Natural Sciences of Philadelphia* 10.
Dalrymple, G.H. 1977. Intraspecific variation in the cranial feeding mechanism of turtles of the genus *Trionyx*. *Journal of Herpetology* 11:255–285.
De Kay, J.E. 1842. Zoology of New York. White & Visscher: 415 pp.
Denton, R.K. Jr, J.L. Dobie, and D.C. Parris. 1997. The marine crocodilian *Hyposaurus* in North America. Pp. 375–397 *in* Callaway, J.M. and E.L. Nicholls (eds.). Ancient marine reptiles. Academic Press, San Diego.
Dollo, L. 1887. On some Belgian fossil reptiles. *Geological Magazine* 4, 392–396.
Esmeray-Senlet, S., K.G. Miller, R.M. Sherrell, T. Senlet, J. Vellekoop, and H. Brinkhuis. 2017. Iridium profiles and delivery across the Cretaceous/Paleogene boundary. *Earth and Planetary Science Letters* 457:117–126.
Evers, S.W., and R.B.J. Benson. 2018. A new phylogenetic hypothesis of turtles with implications for the timing and number of evolutionary transitions to marine lifestyles in the group. *Palaeontology*, online in advance of print. [https://doi.org/10.1111/pala.12384].
Fastovsky, D.E. 1985. A skull of the Cretaceous chelonioid turtle *Osteopygis* and the classification of the Osteopygynae. *New Jersey State Museum Investigation* 3:1–28.
Ferreira, G.S., A.D. Rincón, A. Solórzano, and M.C. Langer. 2016. Review of the fossil matamata turtles: earliest well-dated record and hypotheses on the origin of their present geographical distribution. *The Science of Nature* 103:1–28.
Fichter, L.S. 1969. Geographical distribution and osteological variation in fossil and recent specimens of two species of *Kinosternon* (Testudines). *Journal of Herpetology* 3:113–119.
Fitzinger, L. 1835. Entwurf einer systematischen Anordung der Schildkröten, nach den Grundsätzen der natürlichen Methode. *Annalen des Wiener Museums der Naturgeschichte* 1:103–128.
Fitzinger, L. 1843. Systema reptilium. Braumüller and Seidel, Vindobona: 106 pp.
Gaffney, E.S. 1972. An illustrated glossary of turtle skull nomenclature. *American Museum Novitates* 2486:1–33.
Gaffney, E.S. 1975. A phylogeny and classification of the higher categories of turtles. *Bulletin of the American Museum of Natural History* 155:387–436.
Gaffney, E.S. 1979. Comparative cranial morphology of recent and fossil turtles. *Bulletin of the American Museum of Natural History* 164:65–376.
Gaffney, E.S., H. Tong, and P.A. Meylan. 2006. Evolution of the side-necked turtles: the families Bothremydidae, Euraxemydidae, and Araripemydidae. *Bulletin of the American Museum of Natural History* 300:1–700.
Gallagher, W.B. 1991. Selective extinction and survival across the Cretaceous/Tertiary boundary in the northern Atlantic Coastal Plain. *Geology* 19:967–970.
Gallagher, W.B. 1993. The Cretaceous/Tertiary mass extinction event in the northern Atlantic Coastal Plain. *The Mosasaur* 5:75–154.
Gallagher, W.B. 2003. Oligotrophic oceans and minimalist organisms: collapse of the Maastrichtian marine ecosystem and Paleocene recovery in the Cretaceous–Tertiary sequence of New Jersey. *Netherlands Journal of Geosciences* 82:225–231.
Gallagher, W.B., K.G. Miller, R.M. Sherell, P. Field, and R.K. Olsson. 2011. Vertebrate fossil assemblages and iridium concentrations in the Cretaeous–Paleogene section of New Jersey. *Journal of Vertebrate Paleontology* 31(Supp):113A–114A.
Gentry, A.D., J.F. Parham, D.J. Ehret, and J.A. Ebersole. 2018. A new species of *Peritresius* Leidy, 1856 (Testudines: Pan-Cheloniidae) from the Late Cretaceous (Campanian) of Alabama, USA, and the occurrence of the genus within the Mississippi Embayment of North America. *PLoS ONE* 13:e0195651.
Gilbert, S.F., G.A. Loredo, A. Brukman, and A.C. Burke. 2001. Morphogenesis of the turtle shell: the development of a novel structure in tetrapod evolution. *Evolution and Development* 3:47–58.
Gray, J.E. 1825. A synopsis of the general of reptiles and amphibian, with a description of some new species. *Annals of Philosophy, New Series* 10:193–217.
Gray, J.E. 1831. Synopsis reptilium, pt. 1, Cataphracta: tortoises, crocodiles, enaliosaurians. Treuttel, Wurtz, London: 85 pp.
Gray, J.E. 1834. Characters of two new genera of reptiles (*Geoemyda* and *Gehyra*). *Proceedings of the Zoological Society of London* 2:99–101.
Hay, O.P. 1905. A revision of the species of the family of fossil turtles called Toxochelyidae, with descriptions of two new species of *Toxochelys* and a new species of *Porthochelys*. *Bulletin of the American Museum of Natural History* 21:177–185.
Hay, O.P. 1908. The fossil turtles of North America. *Carnegie Institute of Washington Publication* 75:1–568.
Hirayama, R. 1985. Cladistic analysis of batagurine turtles (Batagurinae: Emydidae: Testudinoidea); a preliminary result.

Studia Geologica Salmaticensia Volumen Especial 1: *Studia Palaeocheloniologica* 1:141-157.

Hirayama, R. 1994. Phylogenetic systematic of chelonioid sea turtles. *The Island Arc* 3:270–284.

Hirayama, R. 1998. Oldest known sea turtle. *Nature* 392:705–708

Hirayama, R. 2006. Revision of the Cretaceous and Paleogene sea turtles *Catapleura* and *Dollochelys* (Testudines: Cheloniidae). *PaleoBios* 26:1–6.

Hirayama, R., and H. Tong. 2003. *Osteopygis* (Testudines: Cheloniidae) from the Lower Tertiary of the Ouled Abdoun Phosphate Basin, Morocco. *Palaeontology* 46:845–856.

Horner, R.J., L.A. Wiest, I.V. Buynevich, D.O. Terry Jr., and D.E. Grandstaff. 2016. Chemical composition of *Thalassinoides* boxwork across the marine K-Pg boundary of central New Jersey, U.S.A. *Journal of Sedimentary Research* 86:1444–1455.

Jalil, N.-E., F. Broin, N. Bardet, R. Vacant, B. Bouya, M. Amaghzaz, and S. Meslouh. 2009. *Euclastes acutirostris*, a new species of littoral turtle (Cryptodira, Cheloniidae) from the Palaeocene phosphates of Morocco (Oulad Abdoun Basin, Danian–Thanetian). *C R Palevol* 8:447–459.

Joyce, W.G., C.J. and Bell. 2004. A review of the comparative morphology of extant testudinoid turtles (Reptilia: Testudines). *Asiatic Herpetological Research* 10:53–109.

Joyce, W.G., J.F. Parham, and J. Gauthier. 2004. Developing a protocol for the conversion of rank-based taxon names to phylogenetically defined clade names, as exemplified by turtles. *Journal of Paleontology* 78:989–1013.

Karl, H.-V., G. Tichy, and H. Ruschak. 1998. *Osteopygoides priscus* n. gen. n. sp., and the taxonomy and evolution of the Osteopygidae (Testudines: Chelonioidea). *Mitteilungen der Abteilung für Geologie und Paläontologie am Landesmuseum Joanneum* 56:329–350.

Latreille, P.A. 1801. Histoire naturelle des reptiles avec figures dissinées d'après nature. Deterville, Paris, 1:1–280.

Lauters, P., Y.L. Bolotsky, J. Van Itterbeeck, and P. Godefroit. 2008. Taphonomy and age profile of a latest Cretaceous dinosaur bone bed in far eastern Russia. *PALAIOS* 23:153–162.

Lehman, T.M., and S.L. Tomlinson. 2004. *Terlinguachelys fischbecki*, a new genus and species of sea turtle (Chelonioidea: Protostegidae) from the Upper Cretaceous of Texas. *Journal of Vertebrate Paleontology* 78:1163–1178.

Leidy, J. 1856. Notices of remains of extinct turtles of New Jersey, collected by Prof. Cook, of the State Geological Survey, under the direction of Dr. W. Kitchell. *Proceedings of the Academy of Natural Sciences of Philadelphi*a 8:303–304.

Leidy, J. 1858. *Hadrosaurus foulkii*, a new saurian from the Cretaceous of New Jersey, related to *Iguanodon*. *Proceedings of the Academy of Natural Sciences of Philadelphia* 10:213–218.

Leidy, J. 1865. Cretaceous reptiles of the United States. *Smithsonian Contributions to Knowledge* 192:1–135.

Lindeman, P.V. 2000. Evolution of the relative width of the head and alveolar surfaces in map turtles (Testudines: Emydidae: *Graptemys*). *Biological Journal of the Linnean Society* 69:549–576.

Linnaeus, C. 1758. Systema naturae, 10th Edition, 1: 824 pp.

Lynch, S.C., and J.F. Parham. 2003. The first report of hard-shelled sea turtles (Cheloniidae sensu lato) from the Miocene of California, including a new species (*Euclastes hutchisoni*) with unusually plesiomorphic characters. *PaleoBios* 23:21–35.

Lyson, T.R., and W.G. Joyce. 2009. A new species of *Palatobaena* (Testudines: Baenidae) and a maximum parsimony and Bayesian phylogenetic analysis of Baenidae. *Journal of Paleontology* 83:457–470.

Matzke, A.T. 2007. An almost complete juvenile specimen of the cheloniid turtle *Ctenochelys stenoporus* (Hay, 1905) from the Upper Cretaceous Niobrara Formation of Kansas, USA. *Palaeontology* 50:669–691.

Matzke, A.T. 2008. A juvenile *Toxochelys latiremis* (Testudines, Cheloniidae) from the Upper Cretaceous Niobrara Formation of Kansas, USA. *Neues Jahrbuch für Geologie und Paläontologie Abhandlungen* 249:371–380.

Myers, T.S., M.J. Polcyn, O. Mateus, D.P. Vineyard, A.O. Gonçalves, and L.L. Jacobs. 2017. A new durophagous stem cheloniid turtle from the Lower Paleocene of Cabinda, Angola. *Papers in Palaeontology* 4:1–16.

Obasi, C.C., D.O. Terry, G.H. Myer, and D.E. Grandstaff. 2011. Glauconite composition and morphology, shocked quartz, and the origin of the Cretaceous(?) main fossiliferous layer (MFL) in southern New Jersey, U.S.A. *Journal of Sedimentary Research* 81:479–494

Owen, R. 1849. Notes on remains of fossil reptile discovered by Professor Henry Rogers of Pennsylvania, US, in greensand formations of New Jersey. *Proceedings of the Geological Society of London* 5:380–383.

Parham, J.F. 2005. A reassessment of the referral of sea turtle skulls to the genus *Osteopygis* (Late Cretaceous, New Jersey, USA). *Journal of Vertebrate Paleontology* 25:71–77.

Parham, J.F., and N.D. Pyenson. 2010. New sea turtle from the Miocene of Peru and the iterative evolution of feeding ecomorphologies since the Cretaceous. *Journal of Paleontology* 84:231–247.

Parham, J.F., R.A. Otero, and M.E. Suárez. 2014. A sea turtle skull from the Cretaceous of Chile with comments on the taxonomy and biogeography of *Euclastes* (formerly *Osteopygis*). *Cretaceous Research* 49:181–189.

Parris, D.C., C. DeTample, and R.C. Benton. 1986. Osteological notes on the fossil turtle ?*Dollochelys atlantica* (Zangerl). *The Mosasaur* 3:97–108.

Prieto-Marquez, A., D.B. Weishampel, and J.R. Horner. 2006. The dinosaur *Hadrosaurus foulkii*, from the Campanian of the east coast of North America, with a reevaluation of the genus. *Acta Palaeontologica Polonica* 51:77–98.

Ramirez, M.D., L. Avens, J.A. Seminoff, L.R. Goshe, and S.S. Heppell. 2015. Patterns of loggerhead turtle ontogenetic shifts revealed through isotopic analysis of annual skeletal growth increments. *Ecosphere* 6:244.

Reynoso, V.-H., and M. Montellano-Ballesteros. 2004. A new giant turtle of the genus "*Gopherus*" (Chelonia: Testudinidae) from the Pleistocene of Tamaulipas, México, and a review of the phylogeny and biogeography of gopher tortoises. *Journal of Vertebrate Paleontology* 24:822–837.

Rivera, G. 2008. Ecomorphological variation in shell shape of the freshwater turtle *Pseudemys concinna* inhabiting different aquatic flow regimes. *Integrative and Comparative Biology* 48:769–787.

Sánchez-Villagra, M.R., and J.D. Winkler. 2006. Cranial variation in *Bairdemys* turtles (Podocnemidae: Miocene of the Caribbean region) and description of new material from Urumaco, Venezuela. *Journal of Systematic Palaeontology* 4:241–253.

Scheyer, T.M., B. Brüllmann, and M.R. Sánchez-Villagra. 2008. The

ontogeny of the shell in side-necked turtles, with emphasis on the homologies of costal and neural bones. *Journal of Morphology* 269:1008–1021.

Schneider, J.G. 1783. Allgemeine naturgeschichte der Schildkröten, nebst einem systematischen Verzeichnisse der einzelnen Arten und zwei Kupfern. Leipzig: 364 pp.

Schweigger, A.F. 1812. Prodromus monographiae Cheloniorum auctore Schweigger. *Arch Naturwiss u Math* 1:271–368, 406–458.

Schwimmer, D.R. 1997. Late Cretaceous dinosaurs in eastern USA: a taphonomic and biogeographic model of occurrences. Pp. 203–211 *in* Wolberg, D.L., E. Stump and G. Rosenberg (eds.). Dinofest International Proceedings. Academy of Natural Sciences of Philadelphia, Philadelphia.

Stephens, P.R., and J.J. Wiens. 2003. Ecological diversification and phylogeny of sea turtles. *Biological Journal of the Linnean Society* 79:577–610.

Tong, H., and R. Hirayama. 2008. A new species of *Argillochelys* (Testudines: Cryptodira: Cheloniidae) from the Ouled Abdoun phosphate basin, Morocco. *Bulletin de la Société Géologique de France* 179:623–630.

Tong, H., R. Hirayama, E. Makhoul, and F. Escuillié. 2006. *Rhinochelys* (Chelonioidea: Protostegidae) from the Late Cretaceous (Cenomanian) of Nammoura, Lebanon. *Atti della Società Italiana di Scienze Naturali e del Museo Civico di Storia Naturale di Milano* 147:113–138.

Turnbull, W.D., and D.M. Martill. 1988. Taphonomy and preservation of a monospecific titanothere assemblage from the Washakie Formation (Late Eocene), southern Wyoming: an ecological accident in the fossil record. *Palaeogeography, Palaeoclimatology, Palaeoecology* 63:91–108.

Ullmann, P.V., and K.J. Lacovara. 2011. Largest known specimen and first mandible of the Cretaceous side-necked turtle *Taphrosphys sulcatus* (Testudines: Pleurodira). *Journal of Vertebrate Paleontology* 31(Supp):207A–208A.

Ullmann, P.V., Z.M. Boles, and K.J. Lacovara. In press. Two new, large specimens of the pleurodiran sea turtle *Taphrosphys sulcatus* from Edelman Fossil Park, Mantua Township, New Jersey. *The Mosasaur*.

Varricchio, D.J., and J.R. Horner. 1993. Hadrosaurid and lambeosaurid bone beds from the Upper Cretaceous Two Medicine Formation of Montana: taphonomic and biologic implications. *Canadian Journal of Earth Sciences* 30:997–1006.

Voegele, K.K., P.V. Ullmann, A. Patel, and K.J. Lacovara. 2012. Insights from a new specimen of the gavialoid crocodilian *Thoracosaurus neocesariensis* from the Maastrichtian–Danian Hornerstown Formation, Sewell, NJ. *Journal of Vertebrate Paleontology* 32 (Supp):190A.

Warner, J.K., X. Combrink, P. Calverley, G. Champion, and C.T. Downs. 2016. Morphometrics, sex ratio, sexual size dimorphism, biomass, and population size of the Nile crocodile (*Crocodylus niloticus*) at its southern range limit in KwaZulu-Natal, South Africa. *Zoomorphology* 135:511–521.

Weems, R.E., and K.M. Brown. 2017. More-complete remains of *Procolpochelys charlestonensis* (Oligocene, South Carolina), an occurrence of *Euclastes* (upper Eocene, South Carolina), and their bearing on Cenozoic pancheloniid sea turtle distribution and phylogeny. *Journal of Paleontology* 91:1228–1243.

Williams, E.E. 1954. A key and description of the genus *Podocnemis* (*sensu* Boulanger) (Testudines, Pelomedusidae). *Bulletin of the Museum of Comparative Zoology* 111:279–295.

Zangerl, R. 1953. The vertebrate fauna of the Selma Formation of Alabama. Part IV. The turtles of the family Toxochelyidae. Fieldiana: *Geology Memoirs* 3:135–277.

Zangerl, R. 1969. The turtle shell. Pp. 311–339 *in* Gans, C., Bellairs, A.D'A. and Parsons, T.S. (eds.). Biology of the Reptilia, vol. 1. Academic Press, London.

Zangerl, R. 1971. Two toxochelyid sea turtles from the Landenian sands of Erquelinnes (Hainaut) of Belgium. *Bulletin de l'Institut Royal des Sciences Naturelles de Belgique Mémoires* 169:1–32.

Zangerl, R. 1980. Patterns of phylogenetic differentiation in the toxochelyid and cheloniid sea turtles. *American Zoologist* 20:585–595.